

# *The Hadley circulation in a changing climate*

Article

Accepted Version

Lionello, P., D'Agostino, R., Ferreira, D. ORCID:  
<https://orcid.org/0000-0003-3243-9774>, Nguyen, H. and Singh,  
M. S. (2024) The Hadley circulation in a changing climate.  
Annals of New York Academy of Science, 1534 (1). pp. 69-93.  
ISSN 1749-6632 doi: <https://doi.org/10.1111/nyas.15114>  
Available at <https://centaur.reading.ac.uk/115307/>

It is advisable to refer to the publisher's version if you intend to cite from the work. See [Guidance on citing](#).

To link to this article DOI: <http://dx.doi.org/10.1111/nyas.15114>

Publisher: Wiley

All outputs in CentAUR are protected by Intellectual Property Rights law, including copyright law. Copyright and IPR is retained by the creators or other copyright holders. Terms and conditions for use of this material are defined in the [End User Agreement](#).

[www.reading.ac.uk/centaur](http://www.reading.ac.uk/centaur)

**CentAUR**

Central Archive at the University of Reading

Reading's research outputs online

# The Hadley Circulation in a changing climate

Piero Lionello<sup>1</sup> | Roberta D'Agostino<sup>2,3</sup> | David  
Ferreira<sup>4</sup> | Hanh Nguyen<sup>5</sup> | Martin S. Singh<sup>6</sup>

<sup>1</sup>DiSTeBA - Dipartimento di Scienze e  
Tecnologie Biologiche e Ambientali,  
University of Salento, 73100 Lecce, Italy

<sup>2</sup>Max-Planck-Institut für Meteorologie,  
20146, Hamburg, Germany

<sup>3</sup>National Research Council, Institute of  
Atmospheric Sciences and Climate, 73100,  
Lecce, Italy

<sup>4</sup>Department of Meteorology, University of  
Reading, RG6 6UR Reading, UK

<sup>5</sup>Bureau of Meteorology, 3008 Melbourne,  
Australia

<sup>6</sup>School of Earth, Atmosphere, and  
Environment, Monash University, 3800  
Melbourne, Australia

## Correspondence

Piero Lionello, DiSTeBA, University of  
Salento, Lecce, 73100, Italy, Roberta  
D'Agostino, Max Planck Institute for  
Meteorology, Hamburg, 20146, Germany  
Email: piero.lionello@unisalento.it;  
roberta.dagostino@mpimet.mpg.de

## Funding information

The Hadley circulation (HC) is a global-scale atmospheric feature with air descending in the subtropics and ascending in the tropics, which plays a fundamental role in Earth's climate because it transports energy polewards and moisture equatorwards. Theoretically, as a consequence of anthropogenic climate change, the HC is expected to expand polewards, while indications on the HC strength are equivocal, as weakening and strengthening are expected in response to different mechanisms. In fact, there is a general agreement among reanalyses and climate simulations that the HC has significantly widened in the last four decades and it will continue widening in the future, but no consensus on past and future changes of the HC strength. Substantial uncertainties are produced by the effects of natural variability, structural deficiencies in climate models and reanalyses, and the influence of other forcing factors, such as anthropogenic aerosols, black carbon, and stratospheric and tropospheric ozone. The global HC can be decomposed

**Abbreviations:** AHT: Atmospheric Heat Transport with AHT(0) denoting its value at the equator; AMIP: Atmospheric Model Intercomparison Project; AMOC: Atlantic Meridional Overturning Circulation; BC: Black Carbon; CMIP: Coupled Model Intercomparison Project; DJF, MAM, JJA, SON: trimesters (December-January-February, March-April-May, June-July-August, September-October-November); DSE: Dry Static Energy; ERA5: ECMWF Reanalysis 5; EFE: Energy Flux Equator; ENSO: El-Niño Southern Oscillation; GHG: Green-House Gases; GMS: Gross Moist Stability; HC: Hadley circulation; ITCZ: Inter-Tropical Convergence Zone; LGM: last glacial maximum; MSE: Moist Static Energy; MSF: Meridional Stream Function; NEI: Net Energy Input; NH: Northern Hemisphere; OHT: Ocean Heat Transport; PIcontrol: PreIndustrial control PDO: Pacific decadal oscillation; PMIP: Paleoclimate Modelling Intercomparison Project; SH: Southern Hemisphere; SST: Sea Surface Temperature; STC: shallow wind-driven Sub-Tropical overturning Cell; TOA: Top-of-Atmosphere

\* All authors share the content of the article, particularly of the final section. PL has coordinated the review. MS, DF, RD and HG have lead sections 2, 3, 4, and 5, respectively.

in three regional HCs, associated with ascending motion above Equatorial Africa, the Maritime Continent, and Equatorial America, which have evolved differently during the last decades. Climate projections suggest a generalized expansion in the Southern Hemisphere, but a complex regional expansion/contraction pattern in the Northern Hemisphere.

KEYWORDS

Hadley circulation, Climate Change, Monsoons, Inter-Tropical Convergence Zone, Expansion, Strength, regional Hadley cells

## 1 | INTRODUCTION

The Hadley circulation (HC) is a global scale atmospheric feature that imports moisture in the tropics and exports energy and angular momentum from the tropics to the sub-tropics, playing a key role in modulating the regional hydrological cycle. The HC consists of two cells, one for each hemisphere, which share an ascending branch in the tropics (the Inter-Tropical Convergence Zone, ITCZ) and have their descending branches in the subtropics. The ascending and descending branches are connected by a flow that in the upper troposphere diverges from the common central ascending branch, exporting energy away from the tropics and in the lower troposphere converges toward the ITCZ, importing moisture.

Variations in the characteristics of the HC are closely associated with those of other global-scale features of the atmospheric circulation, such as monsoons, the mean position of subtropical high pressure systems, the position of jet streams, and the position and intensity of storm tracks. Variations of the HC affect the meridional energy and moisture transport, the tropical and subtropical hydrological cycle and related precipitation regimes at multiple spatial scales [16, 139, 108, 170, 253]. The ascending motion of moist air in the ITCZ is associated with low level convergence, heavy precipitation and deep convective systems, and its structural changes affect tropical precipitation maxima and monsoons [71, 244, 135]. The descending motion is among the mechanisms determining the low precipitation and arid climates found in the subtropics [29, 193]. Consequently, ecosystems, human settlements, agriculture and water resources across the tropics and subtropics are potentially affected by variations in the HC, particularly in monsoon regions and vulnerable semi-arid areas, such as the Mediterranean, the southwestern United States and northern Mexico, southern Australia, southern Africa, and parts of South America and it is expected to influence the future evolution of precipitation in many of these semi-arid regions [197, 22, 50].

Historically, the HC was first detected in surface wind maps in the late seventeenth century by Edmond Halley [92], who sought to explain the observed surface wind convergence in what is now known as the ITCZ as a result of solar heating in the tropics. About fifty years later George Hadley [91] applied the concept of momentum conservation to explain the observed westward surface flow characterizing the subtropical trade winds. Though it took about two centuries to fully appreciate the relevance of those studies and to complement surface with upper troposphere observations [100], the structure of the HC and its dynamics have long been in the background of dynamical meteorology [144, 145]. Studies addressing the characteristics of the HC during past climate conditions when the spatial and



seasonal distribution of the solar forcing was quite different from the present (typically the last glacial maximum, LGM, ~21 kyr BP, and the mid-Holocene, ~6 kyr BP) date back to the 1950's. The interest of the scientific community was increased in the 1970's, when numerical simulation of the atmospheric circulation became feasible [e.g. 242, 21, 116]. In the last few decades, the volume of scientific literature dedicated to studies of the HC has become extremely large [see 59, 152, for an extensive documentation] and in the 2000's the effect of anthropogenic greenhouse gas (GHG) on HC has emerged as a major research topic [192, 188, 110, 185, and subsequent articles cited in this review]. Several review papers have been written on the Hadley circulation (e.g. [204, 15, 149, 217, 216]). Though some overlap between this review and others is unavoidable, our paper aims to provide a distinct contribution as it focuses on the underlying theoretical considerations, it discusses in detail the regional characterization of the HC and it emphasizes both HC width and strength.

The HC is traditionally described using the global Meridional Stream Function  $\Psi(\phi, p)$  [MSF, kg/s 171, 172]:

$$\Psi(\phi, p) = \frac{2\pi R_e \cos \phi}{g} \int_0^p v(\phi, p') dp', \quad (1)$$

where  $R_e$  is the Earth's radius,  $\phi$  is latitude,  $g$  is the gravitational acceleration,  $p$  is the atmospheric pressure and  $v$  is the zonal mean meridional velocity. The global MSF is used to compute properties such as the strength and position of the equatorial ascending branch, the poleward edges of the cells, and the overall HC width. The computation of the MSF using winds provided by profile soundings became possible only in the second half of the 20<sup>th</sup> century. After preliminary attempts in the 1950's, the first reconstructions were completed in the 1960's [175, 232] and by the 1970's reconstructions became sufficiently accurate to allow a monthly climatology [171]. In the late 1990's meteorological reanalyses became available and provided a surrogate of global observations. Instead of using the MSF, some studies have attempted to estimate characteristics and variations of the HC using the surface variables that are affected by it and a variety of different metrics. The HC poleward edges have been identified based on thresholds of the outgoing long-wave radiation [110, 119, 57, 35, 56, 1, 50], the subtropical absolute precipitation minima [112, 35, 36, 50], the zero crossing latitude of the precipitation-evaporation imbalance [147, 119, 57, 52, 1, 56, 217, 50], the zonal-surface-wind zero crossing [10] and the subtropical maxima of the mean sea-level pressure [56, 1, 112, 50]. Proxies of precipitation are often used for geological time scales, including glacial and interglacial cycles and most of the present Holocene epoch [e.g. 157]. However, these variables allow only a partial reconstruction of the full tri-dimensional structure of the HC and some of them poorly correlate with each other [241, 53]. Though some metrics, such as the mid-latitude eddy-driven jet, the edge of the subtropical dry zones, and the Southern Hemisphere subtropical highs exhibit variability and trends consistent with those of the zero crossing latitude of the MSF, others, such as those based on the outgoing longwave radiation, the position of the subtropical jet, the break in the tropopause, and the Northern Hemisphere subtropical highs appear to behave differently [241]. Therefore, metrics other than those based on the MSF are not explicitly considered in this review.

In the annual mean, the global MSF shows two cells, roughly symmetric with respect to the equator, rotating in opposite directions (Fig. 1a). This representation corresponds to the transient condition at the equinoxes, while the solstitial condition exhibits one dominant cell extending from the mid-subtropics in the summer hemisphere to the edge of the subtropics in the opposite winter hemisphere (Fig. 2, [60]). Furthermore, the HC exhibits pronounced regional variability, as trade winds respond to ocean interbasin thermal and moisture flux contrasts [150, 159, 44] and atmospheric flow over land exhibits zonal asymmetries due to surface inhomogeneities and local monsoonal circulations [227, 44]. The global MSF is a smoothed result of the superposition of distinct regional meridional overturning

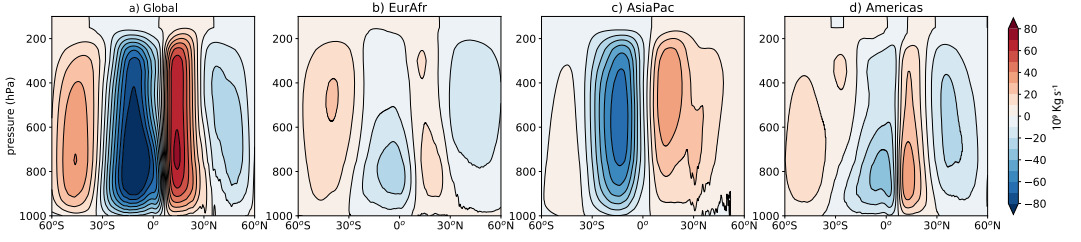


**FIGURE 1** Meridional stream function MSF over the period 1979-2019: global MSF  $\Psi$  (a) and regional MSF  $\Psi_R$  of the Europe-Africa sector (b, EurAfr=20°W-65°E), the Asia-Pacific sector (c, AsiaPac =65°E-140°W) and the sector of the North and South Americas (c, Americas=140°W-20°W). Contour line interval is  $10^{10} \text{ kg} \cdot \text{s}^{-1}$ . All panels are derived from ERA5 [99].

circulations that are the consequence of active convection occurring sporadically in time and space in preferred zones [105, 104].

The decomposition of the global MSF into regional components is based on three conceptual steps. The first step is to decompose the horizontal flow at each pressure level  $p$  into divergent and non-divergent components. Second, the divergent flow is further decomposed in a zonal and a meridional component, which are associated with zonally and meridionally oriented overturnings representing the Walker and the Hadley circulations, respectively. In fact, the local MSF  $\psi(\lambda, \phi, p)$  can be computed for each longitude  $\lambda$  using the meridional component of the divergent flow  $v_d(\lambda, \phi, p)$  and ensuring mass conservation:

$$\psi(\lambda, \phi, p) = \frac{1}{g} \int_0^p v_d(\lambda, \phi, p') dp', \quad (2)$$

which provides a view of the HC whose strength and edges vary continuously with longitude [e.g., 203, 202, 130, 220, 77, 215, 50]. Specifically,  $\psi(\lambda, \phi, p)$  represents a meridional mass flux density, which can be integrated zonally to provide the meridional mass transport across any specified sector. The global MSF can be divided into selected regional MSFs  $\Psi_R(\phi, p)$  by computing the regional zonal average  $v_R(\phi, p)$  of  $v_d$  in selected sectors with a longitudinal angular extent  $\Delta\lambda_R$  [36, 125, 168, 222]

$$\Psi_R(\phi, p) = \frac{\Delta\lambda_R R_e \cos \phi}{g} \int_0^p v_R(\phi, p') dp'. \quad (3)$$

Fig. 1b,c,d shows the resulting regional MSFs for the Europe-Africa, Asia-Pacific, and Americas sectors.

This review considers the HC focusing on aspects that are relevant for understanding the effects of climate change on its characteristics. It does not attempt to review the full body of existing knowledge on the HC, which would not be feasible within a single article. Section 2 describes the theoretical understanding of the HC dynamics [e.g., 97, 234, 208, 101, 90], strength and width (section 2.1), transient behavior and its connection to monsoons (section 2.2.3). Section 3 describes the energy budget of the HC, how it relates to the cross equatorial energy transport and top-of-atmosphere fluxes. Section 4 describes the HC response to different forcings: GHGs, stratospheric and

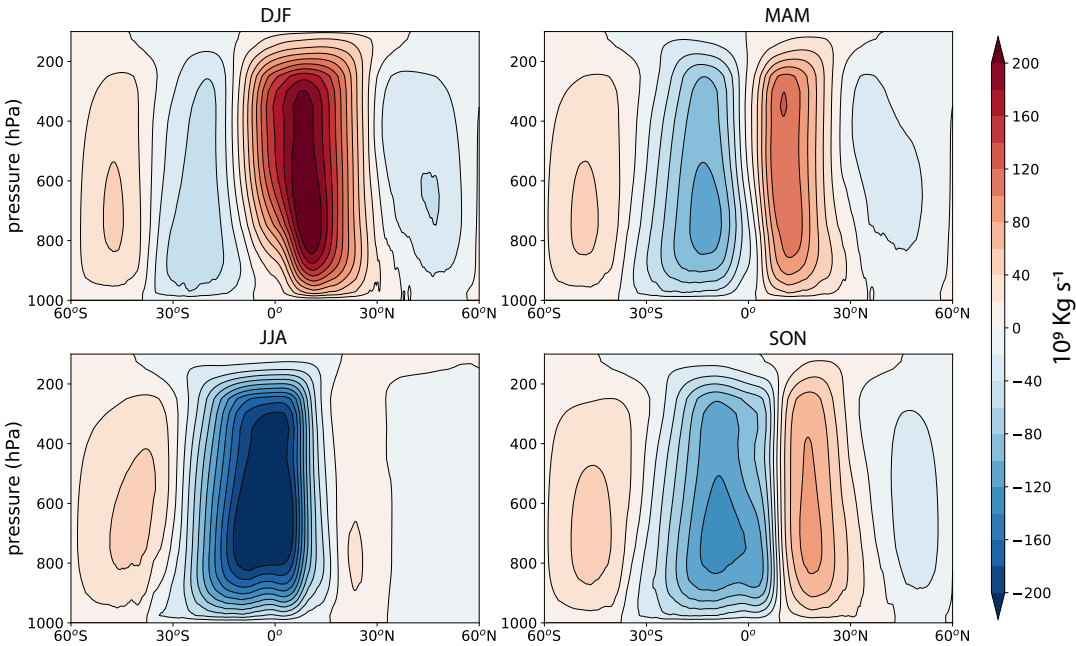


**FIGURE 2** Seasonal cycle of the global MSF over the period 1979-2019 derived from ERA5 [99]. Contour line interval is  $2 \cdot 10^{10} \text{ kg} \cdot \text{s}^{-1}$ . Panels represent seasonal means: DJF (December-January-February), MAM (March-April-May), JJA (June-July-August), SON (September-October-November).

tropospheric ozone, black carbon, dust and volcanic eruptions and astronomical cycles. Section 5 describes how the regional HCs respond to climate change. The status of the knowledge, gaps and present research needs are discussed in section 6.

## 2 | DYNAMICS OF THE HADLEY CIRCULATION

### 2.1 | Scaling of the Hadley Cell

A useful starting point for understanding the dynamics of the HC is the subtropical angular-momentum budget, which expresses a balance between the advection of angular momentum into the subtropics by the mean circulation and the flux of angular momentum out of the subtropics owing to eddies (Fig. 3). An approximate diagnostic for the HC strength may be derived by evaluating this budget for the upper branch at the latitude of the center of the HC [e.g., 234, 201],

$$\Psi_{\text{MAX}}(1 - \text{Ro}) \simeq \frac{S}{f}. \quad (4)$$

Here, the strength of the HC is measured by the MSF maximum  $\Psi_{\text{MAX}}$ , and Ro is the Rossby number of the flow, which may be expressed approximately as  $\text{Ro} \simeq -\bar{\zeta}/f$ , with  $\bar{\zeta}$  being the zonal mean vorticity evaluated in the upper-branch of the HC and  $f$  the Coriolis parameter. The numerator on the right-hand side  $S$  represents net result of the poleward transport of angular momentum provided by eddies integrated vertically between the level of the MSF maximum and the tropopause, and it represents the influence of transient and zonally-asymmetric motions on the HC. Theories of the HC often consider one of two limits: in the axisymmetric limit (section 2.1.1) eddy-momentum fluxes are small and  $\text{Ro} \simeq 1$  [198, 97, 195, 66, 67, 25], in the small-Ro limit (section 2.1.2), the zonal mean vorticity is small compared to  $f$ , and eddy-momentum fluxes are dominant[e.g., 234, 199].

The edge of the HC is usually defined by the latitude of the zero of the MSF at a mid-tropospheric level [e.g., 500 hPa, 75]. In the axisymmetric limit, this latitude is determined not by the angular momentum balance but by the energy budget, under the requirement that the temperature at the cell edge is equal to its corresponding value in the “radiative-convective equilibrium” state in the absence of large-scale circulations [97, 140]. In the small-Ro limit, the angular-momentum budget requires that this latitude coincides with a switch from eddy angular momentum flux divergence to convergence, and the HC edge may be identified as the equatorward margin of wave-activity generation by baroclinic eddies [138]. In this limit, eddies play a central role in determining both the width, as well as the strength, of the HC [96, 234, 138].

#### 2.1.1 | Axisymmetric theory

In the axisymmetric case, the atmospheric flow is assumed to have no zonal variations, the right-hand side of Eq. 4 is zero, and the existence of the HC (i.e.  $\Psi_{\text{MAX}} \neq 0$ ) requires  $\text{Ro} = 1$ . In this case, Eq. 4 becomes degenerate and gives no information about the HC. Nevertheless, the requirement that  $\text{Ro} = 1$  is equivalent to requiring that angular momentum is conserved along streamlines of the flow, and it provides a strong constraint on the zonal wind distribution.

Building on the work of Schneider [198], Held and Hou [97] derived a simple model for the equinoctial HC in the axisymmetric limit (hereafter H&H model), which was extended to the case of off-equatorial thermal forcing by [140].

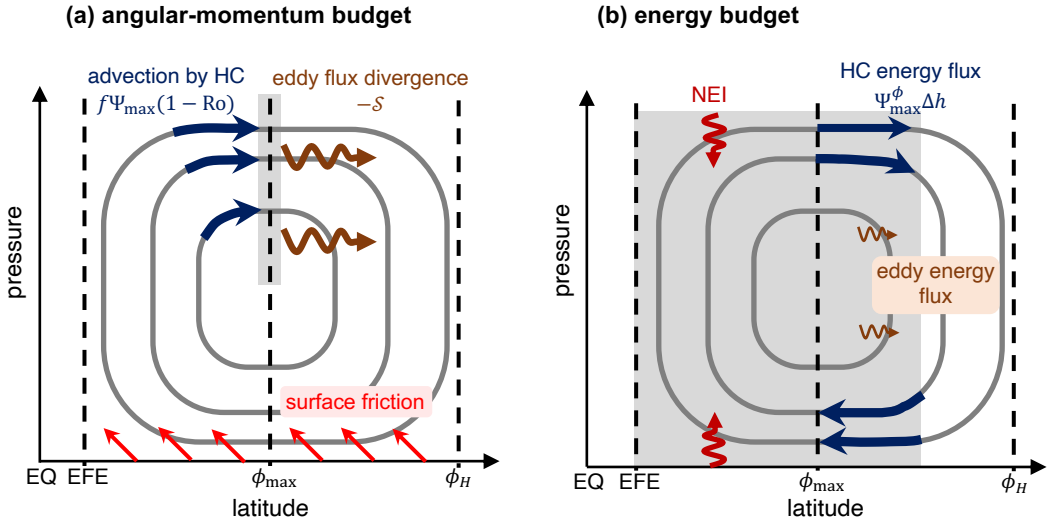


**FIGURE 3** (a) Momentum- and (b) energy-budget constraints on the HC strength. Gray lines represent streamlines of the HC and light gray boxes represent the region over which the budget is evaluated. (a) Angular momentum advection by the mean flow (blue arrows) and eddy angular momentum flux (brown arrows) as considered in Eq. 4. (b) Meridional energy flux by the HC (blue arrows), eddy energy flux out of the tropics (brown arrows) and net energy input (NEI) to the tropical atmosphere (red arrows) as considered in Eqs. 7 and 8. EFE denotes the Energy Flux Equator, i.e., the location where the atmospheric energy transport goes to zero and approximate location of the ITCZ.

The theory relates the angular momentum conserving wind distribution, through the assumption of thermal wind balance and weak surface winds, to the meridional gradient of temperature. Combining this with a simple closure for the energy transport by the cell, a complete description of the HC is obtained. The H&H model predicts a finite width for the HC that, for Earth-like parameters, is comparable to the observed HC width. Moreover, the model provides scalings for the width  $\phi_H$  and strength  $\Psi_{MAX}$  of the HC given by

$$\phi_H \sim \left( \frac{g H \Delta_h}{\Omega^2 R_e^2} \right)^{1/2}, \quad (5)$$

$$\Psi_{MAX} \sim \frac{1}{\tau} \frac{g^{3/2} (H \Delta_h)^{5/2}}{\Omega^3 R_e^2 \Delta_v}. \quad (6)$$

Here  $\Omega$  is the Earth's rotation rate and  $\tau$  is a radiative relaxation timescale. Eqs. 5 and 6 involve parameters that depend on the climate conditions: the troposphere depth  $H$ , the fractional surface-to-tropopause potential temperature  $\Delta_v$ , and a measure of the fractional pole-to-equator potential temperature difference in the "radiative-convective equilibrium" solution that would exist in the absence of a circulation,  $\Delta_h$ . The H&H model (Eqs. 5 and 6) predicts that the strength and width of the solstitial HC increase with increasing tropospheric depth and radiative-convective equilibrium meridional potential temperature gradient, while the strength of the cell decreases with increasing thermal stratification.

### 2.1.2 | Small Rossby number theory

In the small-Ro number limit of Eq. 4, the strength of the Hadley cell is directly related to the eddy angular momentum flux and its divergence in the subtropics. This flux divergence occurs primarily as a result of extratropical baroclinic eddies that form in the mid-latitudes and propagate into the subtropics, where they reach their critical latitude and break, decelerating the mean flow [e.g., 190]. In the small-Ro limit, the HC does not respond directly to the thermal driving, rather, its variations are linked to those of the eddy angular momentum flux divergence in the subtropics [234, 201].

Theories highlighting the effect of eddies on the HC go back to the 1950's when Kuo [131] and Eliassen [65] developed a diagnostic equation connecting the meridional overturning to sources of momentum and heat associated with eddy motions and diabatic effects. A number of authors have also investigated how eddies influence the equinoctial HC by comparing the results of axisymmetric and eddy-permitting simulations of the HC using idealized models [129, 13, 233, 209, 210, 54]. Such comparisons generally reveal that eddies substantially amplify the strength of the equinoctial HC compared to the axisymmetric case, because eddies allow the descending branch to more efficiently lose its angular momentum while approaching the boundary layer. According to Eq. 4, this increases the strength of the HC. However, this amplification is much weaker if the surface temperature is specified instead of being computed by closing the surface energy balance [196, 209]. The strength of the HC has also been found to scale with the magnitude of the divergence of the angular eddy momentum fluxes propagating into the subtropics from the mid-latitudes in a suite of simulations with an idealized GCM over a wide range of parameters [234].

Concerning the width of the HC, it has been suggested that the HC terminates at the location where the axisymmetric solution would become baroclinically unstable [96]. This argument has been supported by both idealized [138] and comprehensive [147] climate change modeling studies, as well as by reanalysis studies of interannual variability

[164], which reveal strong relationships between diagnostics associated with extratropical eddies and the width of the HC [e.g., 124, 128, 26, 218]. Moreover, it is consistent with the observed narrowing of the HC in response to El-Niño [167, 146], which is associated with increased meridional temperature gradients in the subtropics and an equatorward displacement of the storm track.

## 2.2 | The seasonality of the Hadley circulation and its response to climate change

Earth's tropical overturning circulation undergoes an annual cycle where the equinoctial HC, characterized by two cells of roughly equal strength and the ITCZ close to the equator, represents a transitional condition between two solstitial states, each characterized by a strong cross-equatorial HC cell (which has its descending/ascending branch in the winter/summer hemisphere) and a weaker cell in the summer hemisphere [60]. The poleward flow of both equinoctial HC cells and the whole solstitial summer cell occur in regions of upper-tropospheric westerlies, through which mid-latitude eddies are able to propagate. These cells are, therefore, strongly influenced by eddy transports of energy and momentum [234] and are close to the small-Ro regime (section 2.1.2). At the solstices, however, the existence of easterlies in the equatorial upper troposphere prevents Rossby waves from propagating into the deep tropics, limiting the influence of eddies on the HC upper branch [18, 19, 201] and suggesting that axisymmetric dynamics (section 2.1.1) is more relevant for the cross-equatorial solstitial HC. However, eddies still have important effects on the solstitial HC through their effect on the descending branch [23, 24].

### 2.2.1 | The response of the HC width

Motivated by both the axisymmetric theory of H&H and theories based on the onset of baroclinic instability [96], a number of studies have investigated how changes in bulk thermodynamic characteristics of the troposphere under climate change affect the HC width [e.g., 205, 49]. Under global warming, the tropopause height and stability are expected to increase [229], while the meridional temperature gradient in the subtropical atmosphere decreases [2, 205]. Analysis of different climate conditions using PMIP simulations and RCP8.5 projections indicate that, under solstitial conditions, the HC widens as the subtropical static stability and the tropospheric depth increase, while its dependence on meridional temperature gradient differs between the hemispheres [49]. This leads to the relatively robust result that the HC becomes wider as the climate warms [49, 212].

While the above results are qualitatively consistent with the H&H scalings embodied in Eqs. 5 and 6, this should not be taken as a conclusive argument supporting them as all involved variables are correlated among themselves and very well correlated with global warming [49]. In fact, a growing literature suggests that both in equinoctial and solstitial conditions, the HC width is strongly influenced by midlatitude processes [138], scaling with the equatorward-most location at which the mean state is baroclinically unstable [96]. For example, [32] analysed the detailed time evolution of the HC under abrupt 4xCO<sub>2</sub> forcing to show that variations in the subtropical baroclinicity give the best explanation for the simulated shifts in the HC edge. According to this interpretation [e.g., 147, 204, 169], the projected widening of the HC is associated with increased static stability, reduced meridional temperature gradients in the subtropics, and a poleward shift of the storm track [e.g., 185] as seen under La-Niña condition [146]. However, directly relating these changes in the HC width to the influence of eddies or any other external factor remains challenging [2]. Diagnostic relationships between eddy-forcing and shifts in the HC should be cautiously used as an evidence of causality, and the widening of the HC under warming has instead been argued to be an axisymmetric response, with eddies acting as a damping factor to reduce its magnitude [55].

## 2.2.2 | The response of the HC strength

For the strength of the HC, both axisymmetric and small-Ro dynamics may be important, and the relative importance depends on the point in the seasonal cycle being considered. The axisymmetric theory suggests that the HC strengthens with increasing tropospheric depth and meridional temperature gradient, but it weakens with increasing thermal stratification. These scalings, based on the H&H model, have been investigated under different climate conditions using PMIP simulations and RCP8.5 projections [49] showing that the NH solstitial HC strength scales with the tropospheric depth, the fractional pole-to-equator potential temperature difference  $\Delta h$ , and the subtropical near-surface static stability, while a weak and unclear dependence is present for the SH. However, the complex superposition of different responses limits the potential for theoretical constraints on the changes in the HC strength that are produced under future warming scenarios; for example, Chemke and Polvani [30] point out the importance of the direct effect of CO<sub>2</sub> forcing, independent of surface temperature changes. Complicating matters further, idealized simulations suggest that the change in equinoctial HC strength with warming may be nonmonotonic, with changes in eddy fluxes, Rossby number, and ocean heat transport all playing a role [137].

## 2.2.3 | The response of the seasonal migration of the ITCZ

At the solstices, the winter cell dominates the tropical overturning circulation, shifting the zonal mean precipitation maximum into the summer hemisphere and transporting energy across the equator to the winter hemisphere (see section 3). At the same time, monsoon circulations develop over tropical continents, with associated precipitation providing water for over half the World's population [e.g., 187]. While, historically, monsoon circulations have often been conceptualized as large-scale land-sea breezes, with the land-sea contrast considered to be central to their behavior, more recent studies show that monsoons are the regional expression of the seasonal migration of the ITCZ at the solstices [see e.g., 18, 76]. In this view, individual regional monsoons are components of the global monsoon system, and changes in the HC and the global monsoon system are fundamentally coupled [e.g., 80]. Such a view does not preclude a role for land-sea contrasts in influencing the local behavior of individual monsoons [43].

The axisymmetric theory shows that a shift of the thermal forcing maximum by a few degrees from the equator [140] or an isolated, off-equatorial thermal maximum above a low threshold [182] are sufficient to trigger the transition to the regime dominated by a single (winter) HC. Realistic time-dependent cases [67, 233] and observed estimates of the zonal mean circulation [60] show that this transition is less pronounced than in the idealized theoretical description. Further, feedbacks associated with stationary eddies [207, 81] and surface fluxes [17] have a potential role in accelerating the transition between regimes, while surface flux feedbacks and cloud-radiative interactions have a role in the timing and in increasing the rapidity of the onset of the Asian monsoon [151]. A number of recent studies have investigated the sensitivity of the seasonal migration of the ITCZ to the planetary rotation rate [68, 101, 208, 82, 102]. Under climate change, Seth et al. [206] found a delay in the onset of a number of monsoons, attributing this to an increased convective springtime barrier in a warmer world (similar to the so-called upped-ante mechanism [40]). However, detailed understanding of how climate change affects the dynamics of the HC seasonal cycle remains a work in progress [80].



### 3 | LINKS OF THE HADLEY CIRCULATION WITH THE ENERGY BUDGET

The energy budget couples the HC to the net input of energy into the tropical atmosphere by radiative and turbulent fluxes on the one hand, and eddies on the other hand, providing a complementary constraint on the HC strength to the momentum-budget based constraint embodied in Eq. 4 (see Fig. 3). In this section energetic arguments are used to provide a framework to understand the HC response to global warming. Indeed, the primary effect of GHG emissions is to perturb the energy balance at the top-of-atmosphere (TOA), while the thermodynamics and circulation responses work toward re-establishing the energy balance.

#### 3.1 | Meridional Energy transport by the Hadley circulation

Air masses diverging from the ITCZ are drier and cooler than those converging at low level, but they also have significantly higher potential energy. As the latter effect dominates (Fig. 4), the moist static energy (MSE, in J/kg,  $m = C_p T + g Z + L_v q$ , where  $C_p$ ,  $T$ ,  $g$ ,  $Z$ ,  $L_v$  and  $q$  are heat capacity, temperature, gravity, geopotential height, latent heat of vaporization and specific humidity, respectively) of air masses aloft is higher than of those at low levels. The net effect is that, in the vertical integral, the HC exports energy away from the ITCZ while simultaneously importing moisture into the ITCZ. This net meridional energy transport, often described as the atmospheric heat transport  $AHT$ , scales as [95, 45]:

$$AHT(\phi) \simeq \Psi_m(\phi) \cdot \Delta \overline{m}(\phi) + T_e(\phi), \quad (7)$$

where  $\phi$  is the latitude,  $\Delta$  denotes the difference between upper and lower branches of the HC, the overbar denotes the zonal mean,  $\Psi_m$  is the maximum of the global MSF as a function of latitude (kg/s), and  $T_e$  is the eddy meridional heat transport (vertically and zonally integrated). The  $AHT$  is dominated by the overturning term in the Tropics [84] where horizontal gradients, and thus  $T_e$  are small (see Fig. 3).  $T_e$  however becomes dominant away from the Equator. The total  $AHT$  can be decomposed into dry static energy ( $DSE = C_p T + g Z$ ) and latent heat ( $LH = L_v q$ ) transport, which can be obtained (again at the scaling level) as  $AHT_{DSE} \simeq \Psi_m \cdot \Delta \overline{DSE}$  and  $AHT_{latent} \simeq \Psi_m \cdot \Delta \overline{LH}$ , respectively. Since  $LH$ , which depends on the humidity  $q$ , decreases with height while the  $DSE$  increases with height (Fig. 4),  $AHT_{DSE}$  and  $AHT_{latent}$  oppose one another. Using typical values for Earth's atmosphere,  $\Psi_m \simeq 100 \times 10^9$  kg/s and  $\Delta \overline{m} \simeq 10^4$  J/kg, Eq. 7 gives about 1 PW, typical of the  $AHT$  near the peak of the HC MSF [180, 9, 84]. Observations [63] reveal a robust linear relationship between  $\Psi_m(0)$  and  $AHT(0)$  through the seasonal cycle, consistent with a constant value of  $\Delta \overline{m} \simeq 1.4 \times 10^4$  J/kg, emphasizing that, close to the equator, the time (seasonal) variations in  $AHT$  are dominated by changes in the strength of the HC.

$AHT$  is related to the Net Energy Input ( $NEI$ ) in the tropical troposphere, which is given by the vertical integral of the diabatic heating (see Fig. 3) or, equally, the difference between the net radiative fluxes at the top of the atmosphere and net radiative and turbulent fluxes at the surface. In fact, at steady state, the vertically and zonally integrated energy budget of the tropical atmosphere is a balance between the rate at which energy is transported away from the ITCZ (given by the meridional divergence of  $AHT$ ) and the zonally averaged (positive)  $NEI$ :

$$\frac{\partial AHT}{R_e \partial \phi} = 2\pi R_e \cos(\phi) \cdot \overline{NEI}. \quad (8)$$

Using a two-layer description of the atmosphere, [166] connected the  $NEI$  to the vertical motion and energy stratification showing that:

$$NEI \simeq -\frac{\omega_m}{g} \cdot GMS, \quad (9)$$

where  $\omega_m$  (Pa/s) is the vertical velocity at a mid-tropospheric level  $p_m$  separating the upper and lower part of the troposphere. The Gross Moist Stability ( $GMS$ , J/kg) is the difference between the horizontal flow divergence-weighted averaged  $MSE$  of the upper and lower layers and it can be considered a representation of the transport of  $MSE$  away from the tropics by the divergence of the mean circulation. In fact, eq. 9 is a valid approximation only under the assumption that the advection of  $MSE$  by the mean circulation and its transport by eddies are negligible. Physically, Eq. 9 states that, in the deep tropics, where horizontal gradients are weak, ascent ( $\omega < 0$ , a conversion of air parcels from low to high  $MSE$ ) requires a diabatic energy source ( $NEI > 0$ ; see Fig. 3, right panel). However, since the flow is strongly divergent,  $NEI$  can be only partially converted in the  $MSE$  of the upper troposphere, and the concept of  $GMS$  is needed for expressing the relation between  $NEI$  and convection. Eq. 9 loses its relevance away from the equator such that, in the descending branch, the decrease of potential energy and adiabatic warming are balanced by a poleward energy export by eddies (Fig. 3).

The  $GMS$  concept has been extensively used in the subsequent literature and often been redefined [166, 248, 191, 41, 117]. Although all its definitions measure the vertical variations of  $MSE$ ,  $GMS$  has also been interpreted as an efficiency of the meridional heat transport by the HC or a measure of the energy export per unit convective mass flux [103, 243]. Both  $\Delta m$  and  $GMS$  are nearly always positive in the tropical atmosphere [248], because energy is larger in the upper than in the lower tropical atmosphere, though negative  $GMS$  can occur depending on the choice of definition and inclusion, or not, of advection and transient terms (neglected in Eq. 9).

Eq. 9 implies a tight link between changes in  $GMS$  (or  $\Delta m$ ) and changes in vertical velocity:

$$\frac{d\omega_m}{\omega_m} = -\left(\frac{dGMS}{GMS} + \frac{dNEI}{NEI}\right) \simeq -\frac{dGMS}{GMS}, \quad (10)$$

where the second equality is obtained in the limit of small  $NEI$  changes. Eq. 10 provides the link between the strengthening of the stratification and weakening of the overall tropical circulation including the HC. Global warming, on one hand, increases the water vapor concentration in the lower troposphere, therefore reducing  $GMS$ , on the other hand, warms the upper troposphere and uplifts the tropopause, therefore increasing  $GMS$ . The increase prevails so that  $\omega_m$  and the overall tropical circulations weakens (see [39, 41] and references therein). The increase of  $GMS$  and weakening of the circulation, respectively, increases and decreases the energy export out of the tropics (Eq. 7). The two effects roughly cancel out, consistently with the assumption of relatively small  $NEI$  changes in Eq. 10. However,  $NEI$  increases with GHG emissions leading to a small intensification of  $AHT$  (about 0.25 PW at the peak  $AHT$  in both hemispheres [see 148]).

### 3.2 | The ITCZ latitude and cross-equatorial energy transport

Because both vertical  $MSE$  gradient and  $MSF$  are weak at the ITCZ,  $AHT$  is small and changes sign near the ITCZ. In practice, the “energy flux equator” (EFE, where  $AHT=0$ , Fig. 3) is close to the ITCZ, although they are not always collocated [200, 63], because of small, but non-negligible, eddy fluxes in Eq. 7. In the present-day climate the ITCZ is located on average about  $5^\circ N$  and this meridional deviation is most pronounced in the Pacific Ocean [see e.g. 200]. As the distribution of incoming solar radiation is nearly symmetric around the equator, it was suggested this asymmetry was due to land mass distribution and/or ocean-atmosphere coupling [181]. As detailed below, recent studies, using an energy perspective, suggest that the latter effect is the dominant one.

The latitude of the zero energy transport,  $\delta$ , is obtained by a Taylor expansion [200]:

$$AHT(\delta) \simeq AHT(0) + \frac{\partial AHT}{\partial \phi}(0) \cdot \delta = 0, \quad (11)$$

which, using Eq. 8, gives:

$$\delta = -\frac{1}{2\pi R_e^2} \cdot \frac{AHT(0)}{\overline{NEI}(0)}. \quad (12)$$

Using  $\overline{NEI}(0) = 18 \text{ W m}^{-2}$ , and  $AHT(0) = -0.3 \text{ PW}$  [200, 46], one obtains  $\delta \sim 4$  degree of latitude, which is in close agreement with observations. Eq. 12 highlights that the off-equator location of the ITCZ depends on the ratio between the energy transport at the equator (dominated by the HC) and the net energy input. It suggests that a larger  $\overline{NEI}(0)$  would shift the ITCZ closer to the equator at constant  $AHT(0)$ . However, under climate change, both  $\overline{NEI}(0)$  and  $AHT(0)$  are expected to change. Indeed, in  $2\times CO_2$  experiments with slab ocean from CMIP3 (Coupled Model Intercomparison Project 3), [73] found northward/southward ITCZ shifts which are well correlated with decreased/increased  $AHT(0)$ . This is consistent with Eq. 12 although suggesting that  $AHT(0)$  changes dominate over the  $\overline{NEI}(0)$  changes in these experiments.

### 3.3 | Linking the ITCZ position with ocean heat transport, top-of-atmosphere flux and SST

The SH receives about 0.4 PW more than the NH, as the TOA, hemispheric  $NEI$  is positive for the SH (+0.2 PW) and negative for the NH (-0.2 PW) [156, 141]. This asymmetry is dominated by the outgoing long-wave radiation, presumably because the NH is slightly warmer than the SH [136]. The short-wave difference between the two hemispheres is small as they have similar average incoming solar radiation and similar planetary albedo [ $\sim 0.3$ , see 63]. Current best estimates suggest a global ocean heat transport (OHT) of about 0.5 PW northward across the equator [226, 72], which is mostly achieved in the Atlantic basin with a transport of  $\sim 0.7$  PW, while the Pacific Ocean is close to neutral and the Indian Ocean transports  $\sim 0.2$  PW southward (all these estimates have the significant uncertainties of about  $\pm 0.2$  PW). The large Atlantic transport is primarily driven by the Atlantic Meridional Overturning Circulation (AMOC) associated with deep water formation in the Nordic seas and Labrador sea [69]. In the absence of deep water formation in the Pacific and Indian oceans, their transports are dominated by shallow wind-driven sub-tropical overturning cells (STCs). The global northward OHT combined with the 0.3 PW southward transport by the HC balances the TOA radiation asymmetry and closes the energy budget of both hemispheres (Fig. 4).

The hemispheric energy balance suggests that the northward position of the ITCZ compensates for the northward cross-equatorial OHT [156, 74]. This agrees with atmospheric model experiments in which the OHT is prescribed (so-called Q-flux experiments, see [20] and [200] and references therein), where the ITCZ moves northward/southward as the (implied) cross-equatorial OHT is increased/decreased. The ITCZ shift is not seen only in the AMOC-dominated Atlantic sector, but also in the Pacific because of the efficiency of the atmosphere to zonally redistribute the energy output [122]. Variations of the AMOC strength in past and future climates are, therefore, expected to contribute to the displacement of the ITCZ compared to present-day (intensification of AMOC would move the ITCZ northwards and further away from the Equator) [see below 157].

The mechanisms re-establishing the energy balance and connecting the ITCZ to the OHT variations are likely provided by the inter-hemispheric SST difference across the equator that is caused by the AMOC OHT warming the NH and cooling of the SH. A robust linear relationship between ITCZ shifts and changes in interhemispheric tropical SST difference ( $20^{\circ}\text{N} - 0$  minus  $20^{\circ}\text{S} - 0$ , in K) can be found in observations and climate models (with slopes of 3.3 and 3.7 K/deg of latitude, respectively [63]) and under other climates (although with weaker slopes in the range 1.5 - 2.4 K/deg for last glacial maximum, mid-Holocene, and  $2\times\text{CO}_2$ ). Such relationships combined with paleo-proxy estimates of temperature can be used to reconstruct the global ITCZ shifts [157]. Numerical experiments with an imposed cross-equatorial flux demonstrate that the ITCZ is sensitive to high latitude SST perturbations [e.g. 121], possibly generated by AMOC changes [see example in 165] and explained by a "rigidity" imparted to the *AHT* by the weak temperature gradient in the tropics [200]. In climate model projections, the *AHT* anomaly is directed from the faster to the slower warming hemisphere [136].

The STCs and HC are coupled through the wind stress at the air-sea interface ([95], Fig. 4). If the effect of eddy momentum fluxes in the atmospheric boundary layer is neglected, the STC and HC should have opposite mass transports of similar magnitude. However, the STCs are more efficient at exporting heat away from the equator than the HC because the temperature stratification in the ocean is stronger than in the atmosphere [45]. The result is that the coupling between the ITCZ shift and the response of the STCs generates a negative feedback that can limit the excursions of the ITCZ in response to perturbations [85].

## 4 | THE RESPONSES OF THE HADLEY CIRCULATION TO NATURAL AND ANTHROPOGENIC FORCINGS

### 4.1 | HC trends in the last decades

For a long time, behaviors of the HC and interpretation of long term trends in reanalyses were considered uncertain due to the influence of natural variability, which in the late 19<sup>th</sup> and early 20<sup>th</sup> century may have exceeded the changes that occurred in the recent decades [143], and due to different model physics and data assimilation methods adopted by reanalyses [167, 48, 56]. In spite of that, there is general agreement among reanalyses that the global HC has significantly widened in the last four decades, while changes of the HC strength are still uncertain and data-dependent [163, 143, 167, 169, 48, 217, 33, 216].

Fig. 5 compares the HC extension trends in the ERA5 [99] and ERAInterim [58] reanalyses, to those of the CMIP5 and CMIP6 historical "All-forcing" (based on [245]) and preindustrial control (PIcontrol) experiments (based on [87]).

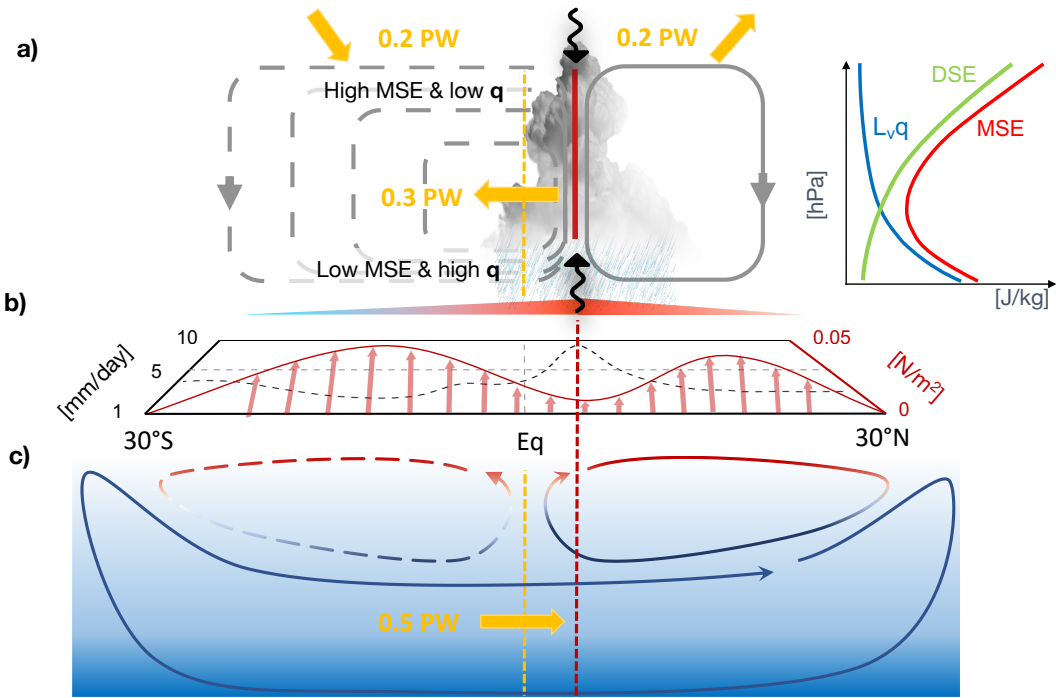


**FIGURE 4** Schematic of the Hadley circulation and associated energy transport. a) Annual mean Hadley cell (grey) and typical vertical profiles of Moist Static Energy, Dry Static Energy and Latent heat. b) schematic meridional profile of precipitation (dashed black line) and surface wind stress (solid red line with arrows). c) Overturning circulation in the ocean showing the Subtropical cells and the Atlantic overturning circulation.

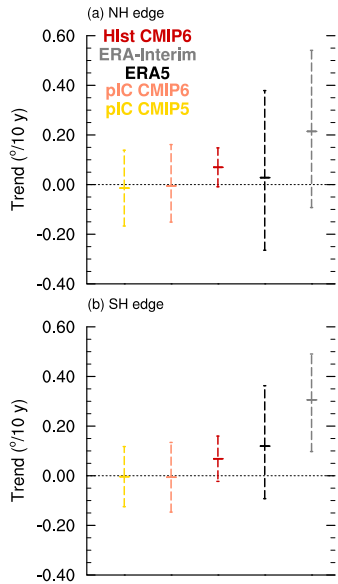


**FIGURE 5** Annual trends of the HC edges in the period 1979 - 2014: for ERA5 (black), ERA-Interim (grey) the central line marks the Sen's estimate and whiskers the 95% confidence interval; for the All-forcing historical simulations (red), the CMPI6 (orange) and CMIP5 (yellow) Plcontrol (piC) the central line marks the multi-model mean value and whiskers indicate the range of possible trends (i.e. twice the inter-model standard deviation,  $2\sigma$ ). Positive/negative trends indicate poleward expansion/contraction of the HC. Units are latitude degrees per decade for the edges (based on [245] and [87]).

The period 1979-2014 is used to avoid the comparison between model simulations and reanalysis before the large increase of satellite data starting in 1979. Though the reanalyses contain structural problems and systematic errors [163, 48, 33], there are indications that these issues do not prevent a realistic reconstruction of the past HC evolution. Fig. 5 shows that the HC expansion in reanalyses (particularly in ERA5) is within the range of models' "All-forcing" experiments [89, 88, 87, 252], with former reanalyses (such as ERAInterim) being just compatible with the largest "All-forcing" trends [8, 2, 169, 48, 87]. This comparison suggests that internal variability has a large impact on long term trends and that structural problems (in climate models and reanalyses) may limit our ability to assess HC trends convincingly [48]. However, by accounting for internal variability and different HC metrics, climate model and reanalysis results can be reconciled [79, 89, 216, 87]. AMIP simulations show that the value of the trends of HC width since the last two decades of the 20th century have been affected by the variability of SST patterns via coupled atmosphere-ocean dynamics [2, 7, 155, 88]. Modes of variability like ENSO and PDO, particularly the change in the phase of the PDO from positive to negative during the late 1990s approximately doubled the rate of tropical expansion from that expected from anthropogenic forcing alone [2, 7, 88]. In fact, Fig. 5 shows that trends of magnitude comparable to those in the reanalyses are present in the Plcontrol simulations as a result of the internal variability alone.

Trends of HC strength and width are caused by the superposition of multiple factors due to internal variability, natural and anthropogenic forcings (e.g. GHGs, stratospheric and tropospheric ozone, aerosols, particularly black carbon, volcanic eruptions and orbital forcing). Disentangling the individual impacts of natural and anthropogenic forcings on

the recent HC evolution is possible by designing single-forcing experiments in an ensemble context. The following subsections discuss the response of HC strength and width to different forcings, highlighting the structural difficulties and consequent uncertainties in CMIP sensitivity experiments in Fig. 6, where, as in Fig. 5, we have considered the period 1979-2014 instead of 1970-2014 originally used in [245]).

The analysis of the impact of various forcings on the HC strength and width that is provided in the next subsections is largely guided by the CMIP experiment prescriptions, i.e. GHG, stratospheric ozone (StratO3), anthropogenic aerosols (Aer) and natural forcings (Nat) as shown in Fig. 6, but it also considers literature on the role of black carbon (BC), tropospheric ozone and the HC response to orbital forcings. Tab. 1 provides a synthesis of the impacts of the considered factors. Results based on dedicated CMIP simulations suggest widening and narrowing of the HC, as a consequence of GHG and anthropogenic aerosols increasing, respectively. In Fig. 6 (updated from [245]) these contrasting effects are pronounced on the SH HC, and not evident in the NH HC. However, the simulations of Fig. 6, may be not fully adequate for describing the role of some factors, such as black carbon and some species of anthropogenic aerosols that have a negligible effect on the global HC, but may be important at regional scale (see section 5.2). Further, the different number of models that were available for the experiments in Fig. 6 (27 for All-forcing, 10 for GHG, 3 for Stratospheric ozone, 9 for Aerosols, 11 for Natural forcing) may affect the relative magnitude of the changes among different experiments, which may not be a function only of the forcings. Moreover, in Fig. 6 individual single forcing trends should not be expected to add up to the "All-forcing" scenario trends, because different subsets of models have been used for each experiment.

For sake of clarity, we restrict the literature review to the aforementioned forcings, although stratospheric aerosol geo-engineering [37], water vapor [246] and Arctic sea ice loss [31], wildfires [225] and natural dust emissions [12] have been proposed to significantly shape the HC too.

## 4.2 | CO<sub>2</sub> and other well-mixed GHG

The large majority of climate model simulations show that weakening of the HC is the prevalent effect of the GHG-induced global warming. In fact, the weakening of the solstitial winter HC is significant in CMIP5 and CMIP6's GHG simulations for the period 1979-2014. There is also consensus on the weakening [41, 147, 230, 49] in climate projections, though with a large uncertainty on its magnitude, ranging between 0 and 4% K<sup>-1</sup> as a function of the global-mean surface air temperature change [147, 49]. The weakening of the HC is qualitatively consistent with the decrease in ascent and associated increase in GMS, as predicted by the simplified energy balance Eq. 10 [sec. 3.1, and 41]. Dynamical theories of the HC do not provide a clear interpretation of the effect of GHG-induced warming on the HC intensity. For instance, according to the H&H model, on one hand, the decrease of the meridional temperature gradient and the increase of vertical stratification in the tropics caused by GHG emission weaken the HC. On the other hand, the increase of the tropospheric depth strengthens the HC (sec. 2.1.1 and references therein).

Model simulations show that that GHG increase leads to HC widening. In the CMIP5 and CMIP6 simulations considered in Fig. 6, the HC expansion driven by GHGs is larger in the SH than in the NH, being significant in the SH in every season, in the NH at the annual scale and in the winter solstitial season. In fact, there is a consensus that GHGs have contributed to HC widening since 1980 in idealized simulations [75, 221, 223, 240] and in the different generations of CMIPs [147, 83, 53, 49, 89, 217, 130, 224, 245, 87, 32] especially in the SH. The asymmetry among

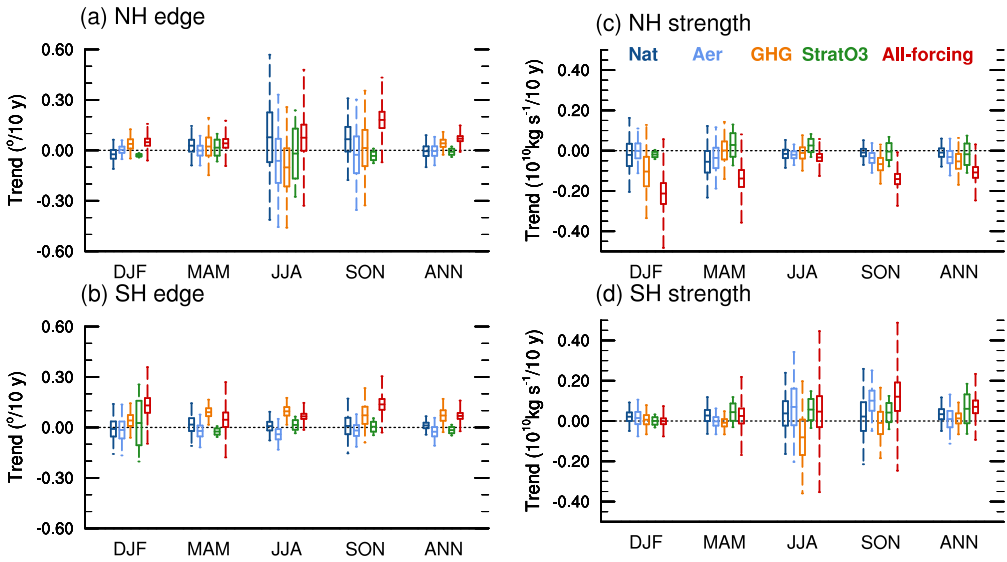


**FIGURE 6** Trends of the HC edges (left) and strength (right) in the period 1979 - 2014 for ERA5 (black), ERA-Interim (grey) and CMIP6 historical simulations: All-forcing (red), GHG (orange), Stratospheric ozone (StratO3, green), Aerosols (Aer, light blue), and Natural forcing (Nat, blue). Positive trends indicate poleward expansion/strengthening and negative trends contraction/weakening of the HC. Units are latitude degrees per decade for the edges and kg/s per decade for the strength. In color whisker-box (CMIP6), the central line marks the multi-model mean value of the trends. Boxes indicate uncertainties on the multi-model mean trends (i.e. twice the standard error,  $2\sigma/\sqrt{n}$ , where  $\sigma$  is the standard deviation of the trends and  $n$  the number of CMIP6 models that have been analyzed in each set of simulations) while whiskers indicate the range of possible trends (i.e. twice the standard deviation,  $2\sigma$ ). Note that the latter is a slight underestimate of the true range of possible realizations as some, but not all, model trends are obtained through ensemble averaging (adapted from [245]).



hemispheres has been highlighted in a set of idealised (quadrupled CO<sub>2</sub> simulations by [240]), who explained it as a result of the smaller sensitivity of the Northern Hemisphere HC to static stability changes. However, seasonal details of Fig. 6 differ with respect to other periods in reanalyses and to climate model simulations, which fail to reproduce the large values found in reanalysis products [2, 48, 87], as natural variability (see the text at the beginning of 4.1) and other factors (see particularly sec. 4.3) need to be taken into account. Further, Fig. 6 is not consistent with the expectation that the GHG effect on the NH HC expansion is larger in autumn (SON) than in other seasons [240]. As this expectation is based on a quadrupled CO<sub>2</sub> concentration [240] and the selection of a different (longer) 1970-2014 period would produce a large HC NH expansion in SON [245], the magnitude of the GHG forcing and of the SST coupling have plausibly a role on this specific seasonal feature. The expansion of the HC is expected in the small-Ro limit, consistent with the northward shift of the storm track and the eddy activity changes (sec. 2.1.2), while the H&H model provide ambiguous indications, as it suggests on one hand an expansion of the HC under GHG forcing, as tropospheric depth is expected to increase, and on the other hand a contraction as the meridional temperature gradient is expected to decrease (sec. 2.1.1).

As in the next decades, without successful mitigation actions, GHG forcing will become dominant, weakening (particularly in the NH, [30]) and widening (particularly in the SH [240]) of the HC shown in climate projections are expected for the future.

### 4.3 | Stratospheric ozone

Stratospheric ozone depletion has been identified as the primary driver of most of SH tropospheric circulation changes in DJF from 1979 until late 1990s [183]. Its immediate effect is to cool the lower-stratospheric polar cap, where the persistent low temperatures and strong circumpolar winds, also known as the polar vortex, prevent meridional mixing and support the formation of a large Antarctic ozone hole. Stratospheric ozone depletion drives the poleward shift of the jet-stream which is intimately related to mid-latitude eddy activity. Therefore, according to the small-Ro theory, the HC strength and width must respond to this specific forcing [186]. Dedicated simulations and CMIP5 and CMIP6 stratospheric ozone experiments [110, 213, 214, 211, 184, 123, 162, 83, 130, 224, 245] simulate widening and modest strengthening of the SH HC in response to this forcing. The relationship between the HC edge and stratospheric ozone concentration found in SH is also seen in the NH in a different set dedicated of model experiments [109]. The SH HC trends have slowed down since the 2000s and this hiatus has been attributed to the recovery of the stratospheric ozone [183, 224, 11]. Therefore, Fig. 6 is not optimal to show the effects of ozone depletion, because the considered period (1979-2014) includes a relatively long sub-period during which ozone recovery occurred. Further, the shown results may not be fully representative, because the number of simulations in the StratO3 experiment is very small. While until the 2000s ozone depletion has contributed to the extension of the SH HC in synergy with GHG increase, its subsequent and future recovery acts in the opposite direction and the overall future evolution of the HC will depend on the net effect of CO<sub>2</sub> and other anthropogenic emissions [183, 224, 11].

### 4.4 | Anthropogenic aerosols, black carbon and tropospheric ozone

In the 20<sup>th</sup> century, anthropogenic aerosols (sulfate, black carbon, organic carbon) have exerted a cooling effect, notably over the industrial areas of the NH, that has partially compensated the GHG-induced warming [27, 28], leading to a global climate evolution quite different from what would have resulted from an increase in GHG concentration alone [136]. The cooling of the NH relative to the SH drives a decrease in the magnitude of the southward energy

transport across the equator and a corresponding southward ITCZ shift [sec. 3.2, and 236, 237, 235, 231] and a deceleration of both SH subpolar and subtropical jets [238]. Since, in contrast to GHGs, past aerosol forcing has warmed the stratosphere and cooled the upper troposphere, it has been suggested that its effect on atmospheric circulation opposes to that of GHGs [194]. In fact, [6] have shown that in the NH the widening associated with the increase in GHGs has been partially offset by the increase of anthropogenic aerosols in the past (when comparing to the preindustrial period, i.e. since 1850), while it is expected to be reinforced during the 21<sup>st</sup> century by the aerosol decrease that will contribute to the poleward shift in the latitude of maximum baroclinicity. However, these estimates strongly depends on whether models include the aerosol indirect effect (mainly on cloud albedo and lifetime), which are subject to uncertainties and aerosol forcings may differ from observations [6]. In the SH the zonal mean circulation changes due to aerosols are not simply opposite to those due to the GHGs [38] and are uncertain [219]. Considering intensity, strengthening of the tropical circulation driven by aerosol-induced NH cooling is consistent with thermodynamic scaling arguments [98]. Considering the last decades of the 20th century, the CMIP6 simulations [245] summarized in Fig. 6 confirm former CMIP5 results [224, 6] that aerosol forcing has had only a minor effect on the HC width, while they show some strengthening of the SH HC that was not present in CMIP5 experiments.

Tropospheric ozone and BC, resulting from the combustion of fossil fuels and biofuels, are both very effective warming agents and have been concentrated over the NH industrial regions for several decades of the 20<sup>th</sup> century, motivating investigation of their combined effects [8]. While tropospheric ozone is not an aerosol itself, its effect can only be reproduced in CMIP-type simulations with an active photochemical module describing its formation where aerosols are involved [86]. Unfortunately, only two models satisfying this requirement are included in the CMIP aerosol experiments shown in Fig. 6 and, further, they share with similar models substantial inaccuracies when compared with tropospheric aerosol observations [86]. Therefore, the representation of the effect of tropospheric ozone in Fig. 6 is possibly poor. The combined effect of BC and tropospheric ozone induces heating of the NH lower troposphere and perturbs the tropical boundary layer moisture, a condition that affects the climate of arid/semi-arid regions [189]. It also contributes to the observed poleward shift of the jet-stream, thereby relocating the main division between tropical and temperate air masses [5, 8]. Sensitivity experiments with a model including a detailed aerosol physics suggest that increases of tropospheric ozone and BC have been the largest contributors to the recent (1979 - 2009) observed widening of the NH HC, having had an effect larger than that of GHG [8].

## 4.5 | Natural forcing: volcanic aerosols and solar irradiance

Large volcanic eruptions inject sulfur particles into the lower stratosphere, where they reflect the incoming solar radiation and absorb solar near-infrared and thermal radiation, producing an overall global cooling effect [132]. The temporary radiative cooling over land (from 1 up to 3 years after the eruption) suppresses clouds, weakens tropical deep convection and the rising branch of the HC, and causes a contraction of the ITCZ [94, 177, 61, 179, 51]. Effects persist for at least two summers after volcanic eruptions [154, 114, 115, 62, 51]. The contraction of the tropical belt and of the HC following major volcanic events is shown by proxy reconstructions over the last 800 years and simulations of the last millennium [154, 42, 142, 4]. Narrowing has been of the order of 0.4-1° in response to Pinatubo-like eruptions and stronger (up to 1.6°) for events of double this magnitude [4].

In CMIP protocols, volcanic eruptions are combined with the solar irradiance variability in the natural forcing experiment (Nat) preventing their disentangling. For the recent decades, CMIP6 Nat simulations do not show any

factor	past decades	projections
GHG	widening and weakening	widening and weakening
Strat O <sub>3</sub>	widening (stronger in the SH)	narrowing (Strat O <sub>3</sub> recovery)
Anthropogenic Aerosols	ITCZ southward shift, uncertain and minor contraction, NH strengthening	depending on aerosol emission
tropospheric O <sub>3</sub>	NH widening (uncertain)	
volcanism	temporary (1-3 years) ITCZ narrowing, uncertain effect on HC width	
ALL	widening, uncertain effect on strength, large role of natural variability	widening (larger in the SH) and weakening (larger in the NH)
glacials	strengthening and narrowing of solstitial circulation	

**TABLE 1** Summary table of the effects of the factors considered in subsections 4.2-4.6

significant change of the HC edges (Fig. 6). However, results of CMIP simulations are uncertain, because the overall effect of stratospheric volcanic aerosol (and of tropospheric dust in general) strongly depends on the prescribed optical properties that can lead to very different, and sometimes opposite, results [161, 3, 251].

#### 4.6 | Orbital forcing and glacial-to-interglacial cycles

The modulation of the distribution of insolation by periodic changes of Earth's orbital eccentricity, axial obliquity and apsidal precession (with periodicities approximately of 100 kyr, 41 kyr and 23 kyr, respectively) in concert with cryosphere and carbon cycle feedbacks [174, 228] drive the Quaternary glacial to interglacial cycles [160, 93, 14]. The complex interplay between orbital forcing, CO<sub>2</sub> concentration, ice-sheet dynamics and ocean circulation have affected the HC strength and width (see sec. 3.2).

During Quaternary interglacials, proxy and modeling evidence indicate orbitally-induced climate conditions different from present day. During the early-to-mid Holocene (9.5 - 6 kyr BP) and the early Eemian (126 kyr BP) interglacials, the NH warming and enhanced interhemispheric insolation and SST gradients in the boreal summer (compared to pre-industrial conditions) presumably led to stronger winter solstitial SH HC and NH monsoons, and a northward shift of the ITCZ, consistent with the relationships found in PMIP models [see sec. 3.2, and 127, 46, 118]. In the boreal winter, models indicate that reduced interhemispheric insolation asymmetries have led to weaker winter solstitial NH HC, SH monsoons and equatorward shift of the ITCZ relative to pre-Industrial [47, 118].

PMIP simulations of LGM (~21 kyr BP) clearly show that the winter solstitial HC was stronger and narrower than in pre-industrial conditions [49, 212]. Literature also provides a consensus on a equatorward shift of the ITCZ [239]. During the glacials and cold episodes, such as the Younger Dryas (12.9 - 11.7 kyr BP) and Heinrich stadials, the complex interplay between orbital and CO<sub>2</sub> forcing, and ice-sheets dynamics presumably led to a AMOC slowdown [78, 70]. Climate model simulations of the Heinrich stadials show decreased northward OHT and an associated equatorward

shift of the ITCZ, weakening of the NH monsoons and a relatively wetter climate in the SH [158]. Similar to other cold periods, reconstructions for the last glacial maximum show a southward shift of the ITCZ [239] and reinforced northeast trade winds [173, 49]. Trade winds proxies of the HC during cold episodes are consistent with the response predicted in section 3.3: cooling the NH relative to the SH shifts the ITCZ equatorward and strengthens the NH trade winds, while it weakens them in the SH [158]. Paleo-proxy and energetic considerations [157] show that the equatorward shift of the ITCZ was likely less than  $1^\circ$  at the LGM [157] suggesting that inferences of large (up to  $4^\circ$ - $5^\circ$ ) shifts from a single proxy may reflect localized changes.

## 5 | REGIONALITY OF THE HADLEY CIRCULATION

Section 4 highlighted the hemispheric asymmetry as well as regional impacts of different forcings on the HC. This suggests that changes or absence of changes in the global HC due to a specific forcing may result from a combination of additive or competing regional effects. Therefore, the global perspective is likely to miss important regional changes (addressed in this section) that have important environmental effects on precipitation and droughts.

### 5.1 | Characteristics of the regional Hadley circulations

The HC shown in Fig. 2 does not resemble the circulation at any given longitude. Areas of ascent do not spread uniformly around the globe, rather they are strongly localized [202, 168]. The seasonal cycle of the local MSF  $\psi(\lambda, \phi, p)$  at  $p = 500$  hPa (Fig. 7, left panel) shows three centers of minima in the SH and maxima in the NH located near the equator above Africa, the Maritime Continent and America. These minima/maxima in each hemisphere are meridionally separated by the zero contours of the MSF near the equator, which are associated with intense ascent and where the meridional gradient of  $\psi$  is strongest, concomitant with the ITCZ. The regions of intense ascent are zonally separated by a discontinuity near  $60^\circ\text{E}$ ,  $140^\circ\text{W}$  and  $20^\circ\text{W}$  and are marked by seasonal and regional variability. The strongest center is located above the Maritime Continent in the solstitial seasons and the weakest above Africa in the equinoctial seasons.

Wherever there is a tropical monsoon regime associated with deep convection and rising motion near the equator and descending motion in the subtropics, with equatorward flow near the surface and return flow in the upper troposphere, it is possible to define a regional HC [107, 106, 47]. This motivates a regional perspective of the HC where Eq. 3 is used to define  $\Psi_R(\phi, p)$  for three different regions (AsiaPac, EurAfr, Americas, Fig. 1) characterized by different morphology, land-sea patterns, monsoonal flow and seasonally varying ITCZ [168]. This regionalization is consistent with a recent theoretical framework that describes the HC as the results of active tropical convection occurring over specific zones (Equatorial Africa, Indian Ocean and west Pacific, east Pacific and Equatorial America) and enhanced during certain periods causing meridional circulations on longitudinally confined sectors [107, 106]. All three regional HCs (Fig. 1b-d) exhibit an overturning structure in both hemispheres, but with marked regional variability, which is associated with the different strengths of their respective ITCZ and rising branch (Fig. 7). The AsiaPac HC is the strongest, while the EurAfr HC is the weakest. The width of the cells differs among the three regions especially in the NH where the AsiaPac cell extends far beyond the subtropical latitudes due to the strong Asian summer monsoon [107]. This is consistent with other studies that have described the zonal variations of subtropical margins using different metrics [50, 216]. The results shown in Figs. 7 (left panel) and 8 have been obtained using the most recent ECMWF reanalysis product ERA5 for the period 1979-2020 and confirm that the AsiaPac is stronger and wider than

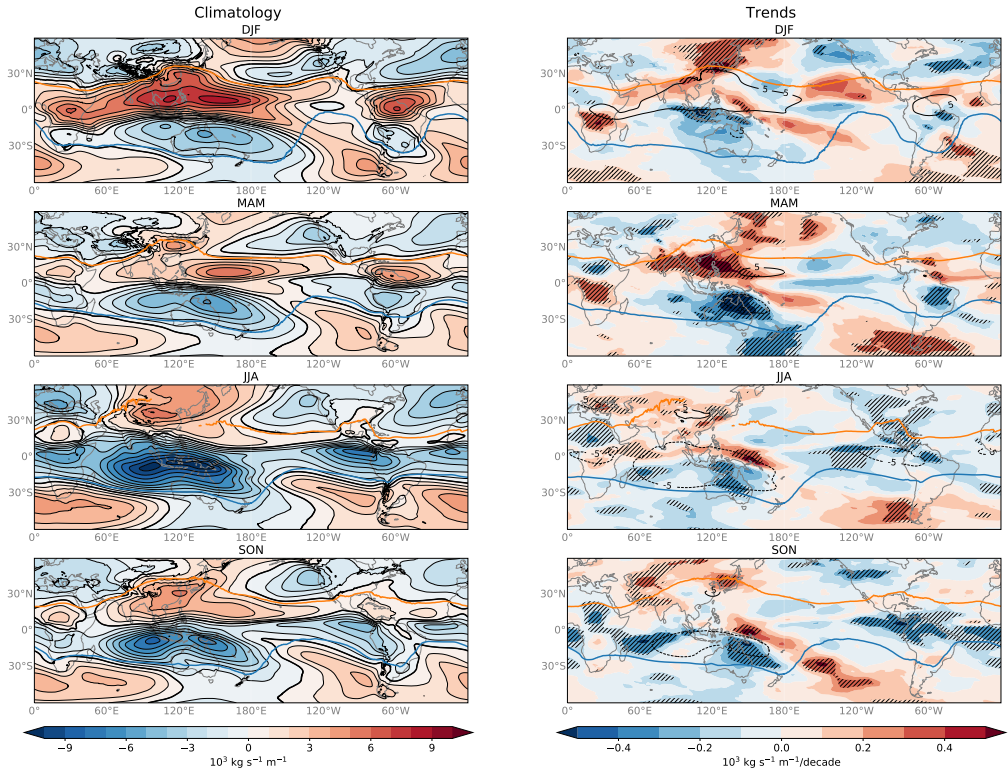


**FIGURE 7** Seasonal cycle of the local MSF at 500hPa (left) and their long term trend (right) derived from the ERA5 divergent meridional wind over the period 1979-2020. In the left column panels the zero-contour is highlighted in black. In the right column panels hatched areas denote values statistically significant to the 95% level and black solid/dashed contours show the  $\pm 5 \times 10^7 \text{ kg s}^{-1}$  MSF levels. In all panels thick orange and blue lines indicate the local edges of the overturning circulation when they can be defined.

the other two HCs. The main features and the magnitude of the local MSF in the Asia-Pacific, Europe-Africa, America sectors and their seasonal variations are similar if a different (e.g., 1970-2014) period or the former ERA-Interim reanalysis are adopted and are consistent with analogue published climatologies [215].

The intensity of the regional HC can be defined as the maximum of  $\Psi_R(\phi, p)$  between the equator and  $30^\circ$  latitude and its edge as the latitude where  $\Psi_R(\phi, p)$  is decreased to 25% poleward from its maximum value averaged between 400 - 700 hPa [168]. Though this threshold is subjective, its value is not critical and reducing it (e.g. to 10% as in [215]) does not appreciably affect the results. The methodology adopted in Fig. 7 fails to identify the edge of the HC NH only in the Asia-Pacific sector in the boreal summer in a zone around the west coast of the Pacific Ocean, but, depending on the adopted methodology the definition of the HC edges may fail at several longitudes [215]. However, results are generally consistent at the longitudes where the edges are identified by the different methods and datasets. The seasonal cycle of the edge and intensity of the regional and global HC are presented in Fig. 8. Both the edge and intensity of the regional HCs loosely follow the annual cycle of the global HC. According to the maps of the local MSF at 500 hPa (Fig. 7), in the NH between May and August the (summer solstitial) AsiaPac has

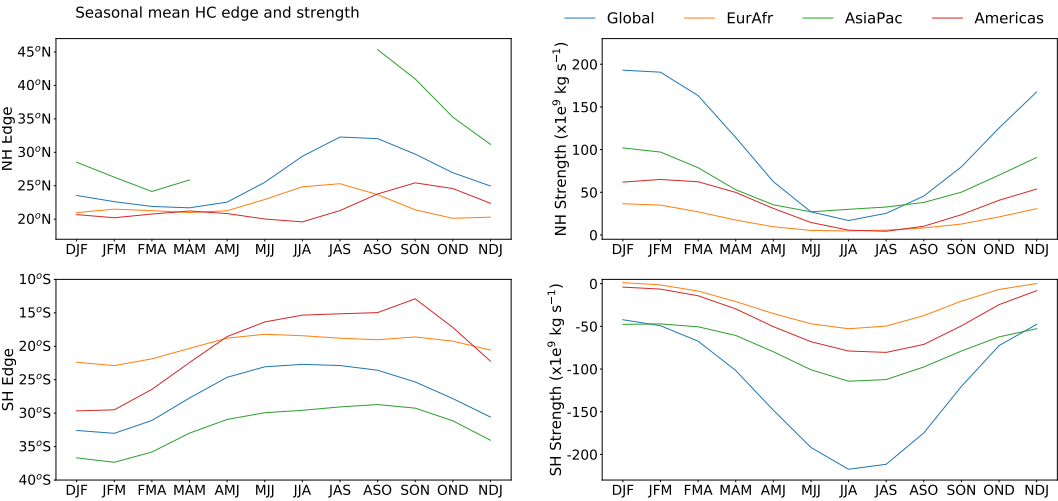


**FIGURE 8** Seasonal cycle (3-month running average) of the edge (left, in degrees of latitude) and strength (right, in  $\text{kg s}^{-1}$ ) of the three regional and global HCs for the Northern (top, NH) and Southern (bottom, SH) Hemisphere according to ERA5 and the 1979-2020 period. The regional HCs are Europe-Africa (EurAfr;  $20^{\circ}\text{W}$ - $65^{\circ}\text{E}$ , orange), Asia-Pacific (AsiaPac;  $65^{\circ}\text{E}$ - $140^{\circ}\text{W}$ , green) and Americas (Am  $140^{\circ}\text{W}$ - $20^{\circ}\text{W}$ , red). Missing values in the summer months for AsiaPac NH edge are due to the cell extending to the pole.

no well defined northern limit. The occurrence of the maximum (minimum) extension of the Americas NH (SH) HC during the autumn (spring) equinoctial conditions might be an artifact caused by the criterion used for defining the edges; in this case the HC is weak and its regional extension has an irregular shape. Note that the weighted average of the regional edges equals the global edge and the sum of the regional intensities equals the global intensity (Fig. 8).

## 5.2 | Past and projected changes of the regional Hadley circulations under anthropogenic climate change

Here, we discuss changes of the HC that are marked by regionality and seasonality [e.g., 202, 50, 215] using the ERA5 data for the period 1979-2020 to support the discussion<sup>1</sup>.

Fig. 9a shows the trends of the HC poleward edges adopting a 95% significance level. Global expansion is driven by the Asia-Pacific HC, which is the unique sector presenting positive values in all seasons and in both hemispheres, while in the Europe-Africa and America sectors most values are negative. The statistically significant global expansion of the winter solstitial and autumn equinoctial SH HC results from non significant trends that are positive in all sectors in winter, but only in the Asia-Pacific HC in autumn. At the annual scale, the statistically significant expansion of the SH HC results from the positive trend in the Asia-Pacific sector, only partially reduced by narrowing (statistically non significant) in the America sector. There are no statistical significant trends of the NH HC

<sup>1</sup>These data and results have not been previously published.

Fig. 9b shows strengthening of the HC, which is more robust in the SH than in the NH. The SH HC strengthening is driven mostly by the intensification in the Asia-Pacific sector, which is significant in all seasons but summer. In the NH, weakening of the Europe-Africa and America sectors contrasts the strengthening of the Asia-Pacific sector in all seasons, leading to a significant weakening of the summer solstitial global NH HC. The agreement with [215] is partial as their results show HC strengthening in the America sector in all seasons.

Therefore, Fig. 9 shows that the HC expansion and strengthening in the period 1979-2020 have not been zonally uniform, but actually contraction and weakening have occurred in many seasons for the Europe-Africa and America sectors. Further, natural variability prevents identifying statistically significant trends at regional scale in most sectors and seasons.

Breaking down the HC regional changes of Fig. 9 to longitudinal scale by the analysis of the local  $\psi(\lambda, \phi, p)$ , (Fig. 7, right panel) allows one to interpret the trends in Fig. 9 in terms of sub-regional features. In most season, the expansion and strengthening of the AsiaPac SH HC is driven by its behavior over the Maritime Continent. The intensification of the winter SH HC in the Americas sector is reflected in a significant signal over south America and the East Pacific in Fig. 7, while the interpretation of the trends over equatorial Africa is less clear. Many features that are present in [215] are confirmed in Fig. 7 right panel, but in Fig. 7 the intensification of the HC above America and the Indian Ocean in JJA are weaker and have a different spatial structure than in [215]. Further, [202] shows SH winter solstitial trends different than in [215] above equatorial America and do not exhibit the significant intensification of the Asia-Pacific SH HC that is evident in Fig. 7, right panel. These disagreements can be partially explained by the different periods that have been adopted (1979-2017 for [215], 1979-2009 for [202], 1979-2020 for Fig. 7), as these trends are strongly affected by natural variability [89, 215], but it is also likely that structural issues can locally cause substantial differences between re-analyses (namely between ERA-Interim and ERA5).

Beside land-sea contrast and ocean circulations, a major role in the lack of zonal uniformity of past evolution of the HC is played by aerosol emissions, whose major sources have moved in the last few decades from North America and Western Europe to East Asia and tropical regions. In the regions of strong convection such as in monsoon areas and the ITCZ, the BC-induced surface cooling and tropospheric warming could have masked the effect of GHG forcing, and may have been responsible for regional impacts, such as Sahel drought, Indian monsoon weakening and meridional shift of the East Asian rainfall pattern observed in the mid-20<sup>th</sup> century. In arid and hyper-arid areas collocated with the HC descending branch, the overall BC effect could have contributed to expansion of the subtropical dry zones and local increase of drought intensity [189, 8, 111].

Dust, which has not been included in CMIP aerosol prescriptions [189], absorbs solar radiation and absorbs/re-emits thermal infrared radiation [126] exerting a large influence on the energy budget of the dry subtropics, such as the Saharan and Arabian deserts. Over North Africa, the dust radiative effect strengthens the NH HC, inducing a slight northward shift of the ITCZ and increased precipitation [12]. However, global climate model simulations show a contrasting response of the tropical rain belt to dust forcing [247, 133, 249, 250]. The disagreement may arise from uncertainties associated with different representation of dust optical properties, with large absorption producing a large negative net radiative effect and a positive impact on the hydrological cycle. On paleo-time scales, dust follows the long-term oscillations associated with glacial-interglacial cycles. During interglacial humid and more vegetated periods, such as the mid-Holocene, the HC is wider and stronger [49]. The dust reduction over the "Green Sahara" strengthens the vegetation-albedo feedback, increasing further the area and intensity of the African monsoon and



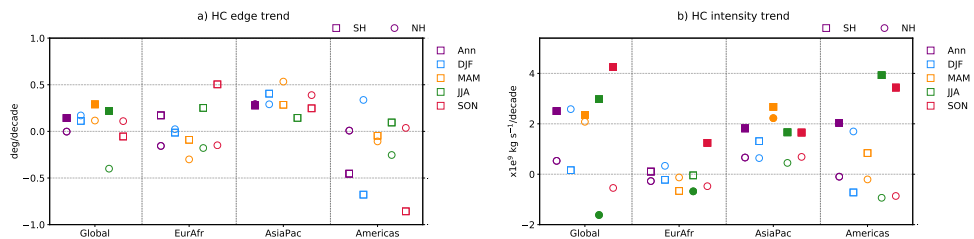


**FIGURE 9** ERA5 1979-2020 annual and seasonal trends in the edge (panel a) and strength (panel b) of the zonal mean and regional HCs. Trends in the NH/SH are indicated by open circles/squares, with values statistically significant (at the 95% confidence level) indicated by filled circles/squares. Positive values indicate expansion/strengthening.

the local HC [178].

CMIP6 projections under the combined SSP3.0-RCP7.0 scenario show a northward shift of the ITCZ over eastern Africa and the Indian Ocean and a southward shift in the eastern Pacific and Atlantic Oceans and South America associated with changes in the divergent atmospheric energy transport by 2100 [153]. These shifts appear to be associated with meridional SST contrasts; in the Indian Ocean higher SST warming is located in the northern subtropics while in the eastern Pacific and Atlantic Oceans it is located between 10°S and 5°N. The South Atlantic Convergence Zone is projected to shift southward in association with the deepening of the south Atlantic subtropical high [176], while over Africa the ITCZ is projected to shift northward associated with the deepening of the Saharan heat low [64].

The multi-model mean local  $\psi(\lambda, \phi, p)$  weakens significantly at most longitudes [215] in an ensemble of simulations of CO<sub>2</sub> quadrupling. However, the widening signature is more complex. In the NH for the winter solstitial HC, widening is projected over the Middle East and the Western Pacific, while contraction is projected over Southwest America, North Atlantic and East Asia [see also 47]. The autumn widening of the equinoctial NH HC over east Pacific and Middle East results in a small NH HC widening. In contrast, SH widening is projected in all four seasons but is largely driven by widening over the East Pacific where the overturning circulation is weak. In summary, the projected regional effects of increasing GHG concentration and the trends in reanalyses present large discrepancies, that make the attribution of regional changes of the HC edges since 1979 to anthropogenic climate change problematic. The analysis of [50] suggests that the anthropogenic expansion of the tropical belt will emerge within this century only in few areas of the NH (the Mediterranean/Middle East and, to a lesser extent the Western Pacific).

## 6 | DISCUSSION AND CONCLUSIONS

Theoretical understanding of the HC dynamics generally considers the axisymmetric limit, in which eddies are not considered, and the eddy-driven small-Ro limit, in which extratropical processes strongly constrain the HC. In Earth's HC, the relevance of these limits is expected to differ at different points of the seasonal cycle. The axisymmetric scaling provided by the H&H model [97] represents a theoretical framework for the solstitial winter HC, since its response to the off-equatorial solar forcing is weakly influenced by eddies. The small-Ro limit [131, 65, 199] represents a theoretical framework more suitable than the axisymmetric theory for understanding the HC during equinoctial conditions,



when its extension is associated with the activity of the mid-latitude eddies (controlled by the Eady growth rate) and the position of the storm track. In spite of theoretically different conditions for their validity, both frameworks have been applied in general to the HC. However, recent studies, which evidence the relevance of mid-latitude processes (and therefore of the small-Ro limit) both in equinoctial and solstitial conditions, suggest that the axisymmetric theory is not relevant for the HC width [138, 32].

The axisymmetric theory suggests that both HC width and strength increase with the troposphere depth and radiative equilibrium meridional temperature gradient, and that the strength also decreases with the thermal stratification in the tropics (sect.2.1.1). Small-Ro theory implies that the width is sensitive to changes in baroclinicity in the subtropics, implying that the latitude of the HC edge shifts consistently with the meridional position of the mid-latitude storms track, and the HC strength is related to that of the eddy momentum flux divergence in the subtropics, implying that it varies with the intensity of the mid-latitude eddies (sect.2.1.1).

Climate projections, largely driven by the radiative effects of the increasing GHG concentration, show significant expansion and weakening of the HC, which are consistent with the role of the troposphere depth and of the subtropical near-surface static stability, respectively [e.g., 147, 120, 224, 134, 49, 87] and/or increased static stability in the ascending branch with differences among the NH and SH [32, 30]. Since the parameters of the H&H scaling vary with global warming, the H&H model can be used to support the extension and weakening of the HC with the intensity of the anthropogenic climate change identified in PMIP3-CMIP5 numerical experiments [49]. The expansion of the HC is also supported by the small-Ro theoretical limit through the poleward migration of the storm track, increased static stability, and reduced meridional temperature gradients in the subtropics resulting from anthropogenic global warming [147, 185, 146, 204, 169]. These are the bases for the expectation of the future expansion and weakening of the winter HC, but with uncertainties on their magnitude, so that the climate change signal might not emerge from natural variability in the NH during the 21st century even in a high emission scenario [88].

Energy budget considerations suggest that the tropical circulation weakens in response to the increase of gross moist stability of the tropical troposphere, but strengthens with increasing  $NEI$ , which are both effects caused by increasing GHG concentration. Climate models generally favour a decrease in HC strength with warming, although a strengthening cannot be ruled out either based on models or theoretical considerations, limiting the confidence on the future weakening of the HC.

Historical climate simulations and meteorological reanalyses suggest that an expansion of the HC has occurred in the recent decades (particularly of the winter solstitial HC). The quantitative agreement among the two sets of data is poor, with substantially smaller trends in simulations than in reanalyses [e.g., 110, 112, 113, 167, 169, 48, 245], but they can be reconciled accounting for the large role of natural variability that has approximately doubled the rate of tropical expansion from that expected from anthropogenic forcing alone [2, 7, 88]. Changes in the HC strength and their interpretation are uncertain. The HC has been mostly weakening in historical simulations of GHG [245] but mostly strengthening in reanalyses (as it is shown also the ERA5 data considered in this article) particularly in the SH. Using sea-level pressure gradients to estimate the change of the HC strength, [34] suggested that the NH HC has weakened over recent decades, and the weakening is attributable to anthropogenic emissions. The proposed explanations for these disagreements include structural climate model deficiencies, multidecadal variability [56, 252] and/or possible artifacts in the reanalyses [48]. In general, there is a growing evidence that properly accounting for natural variability, climate model and reanalysis results can be reconciled [89, 216, 79, 252] and, though the reanalyses

contain structural problems and systematic errors [163, 48, 33], these issues do not prevent a realistic reconstruction of the past HC evolution.

Variations of the HC are linked to multiple factors that have played a role in the recent decades. The widening caused by increasing GHG concentration, has been further amplified by the contribution of the stratospheric ozone depletion (at least in the SH). The NH cooling produced by anthropogenic aerosols is expected to have exerted an effect opposite to GHGs that occurred mostly in the NH, but there are large uncertainties in the estimates of their individual effects. Solar irradiance and volcanic forcing in the 20<sup>th</sup> century have not produced any significant trend of the HC in climate simulations. In synthesis, there is a consensus among theoretical arguments, reanalyses and climate model simulations that an expansion of the global HC has occurred in the recent decades, and that increasing GHG concentration and stratospheric ozone depletion have contributed to it. Consistently with these mechanisms, climate models project robust future HC expansion in the SH (but not in the NH), and robust future HC weakening in the NH (but not in the SH) as a result of the GHG increase and the recovery of stratospheric ozone (e.g. [30]).

Energy budget considerations provide a background for understanding variations of the strength of the *AHT* and of the shift of the ITCZ, which are relatively recent topics (e.g. they were not highlighted in [59]). The annual mean location of the ITCZ north of the equator and the associated southward atmospheric heat transport at the equator are consolidated features across different climates and in recent times. This is caused by the large northward OHT across the equator overcompensating for different signs of the TOA energy budget of the two hemispheres. Anthropogenic climate change is expected to increase *NEI* in the tropics and, therefore, to simultaneously shift the ITCZ equatorwards and increase the *AHT*. The magnitude of both effects is uncertain.

During the last 15 years, regional aspects of the HC have gained relevance as the global perspective has revealed its limitation for the full understanding of recent, past and future trends of the HC. A measure of this progress could be the comparison of the discussion in this article with respect to [59], published in 2004, where the importance of regional features had only begun to emerge. In fact, the global HC concept hides the fact that both ascending and descending motions are not zonally uniform and are concentrated above the three areas: Equatorial Africa, the Maritime Continent and Equatorial America. While these three regional features, particularly the HC above the maritime continent, can be clearly identified in all seasons, the HC and an overturning circulation do not exist at all longitudes and seasons (e.g. in the central Pacific) and the identification of the edges might fail depending on the adopted method.

The identities of regional HCs and their different behaviors have become clear, also in terms of different past and future responses, including responses to forcings with regional characterizations (black carbon, volcanic and anthropogenic aerosols, tropospheric and stratospheric ozone) and regional responses to globally homogeneous forcing (anthropogenic GHG). The expansion of the Asia-Pacific circulation in the SH has been the dominant signal in the last few decades and is expected to play the same role in the future. Further, the OHT variations in the different ocean basins can determine zonal variations of the ITCZ shift whose sign may change depending on the basin. In fact, simulations show a future northward shift of the ITCZ over Africa and the Indian Ocean, southward over the Atlantic, eastern Pacific and Americas. The large differences between the regional responses of the HC to GHG and the trends observed in reanalyses in the last 40 years, makes the attribution of its recent regional evolution to anthropogenic climate change problematic [215], and the signal might need several decades to emerge at regional scale, particularly in the NH [50]. Reducing the existing uncertainties on regional responses of the HC to increasing GHG and other factors is presently problematic because there are multiple forcing agents present with contrasting effects and likely

strong model-dependency of results, which have shown major limitations in reproducing the regional evolution of the HC in the last decades.

Though the present theoretical understanding provides useful guidelines, interpretation of past variations (particularly at the regional scale) is still in part uncertain. CMIP5 and CMIP6 simulations do not capture well HC, ITCZ and precipitation changes suggesting the need of reducing structural model uncertainties. However, important progress has been obtained explaining a substantial fraction of recent trends to multidecadal natural variability. A possible way forward to better connect theory to observation and simulations would be to unify the energetic and momentum-based perspectives discussed in sections 2 and 3 to a more coherent theory for the HC. Further, an important direction for future work is to develop theoretical constraints on regional HCs.

## Acknowledgements

Roberta D'Agostino was funded by the Deutsche Forschungsgemeinschaft (DFG, German Research Foundation) under Germany's Excellence Strategy – EXC 2037 Climate, Climatic Change, and Society (CLICCS) - Cluster of Excellence Hamburg, A4 African and Asian Monsoon Margins – Project Number: 390683824.

Martin Singh acknowledges funding from the Australian Research Council through grants DE190100866, DP200102954 & CE170100023. Authors acknowledge Yan Xia and Yongyun Hu for providing data for producing Fig. 6.

The authors are very grateful to Prof. Kevin Grise for the data pre-Industrial control data shown in Fig. 5 and to Dr. Yan Xia for the data shown in Fig. 5 and 6. We are indebted to an anonymous reviewer for comments and suggestions that have substantially contributed to the quality of this review article.

## Competing interests

The authors have no competing interests to disclose.

## references

- [1] Adam, O., K. M. Grise, P. Staten, I. R. Simpson, S. M. Davis, N. A. Davis, D. W. Waugh, T. Birner, and A. Ming, 2018: The TropD software package (v1): standardized methods for calculating tropical-width diagnostics. *Geoscientific Model Development*, **11**, no. 10, 4339–4357, doi:10.5194/gmd-11-4339-2018.
- [2] Adam, O., T. Schneider, and N. Harnik, 2014: Role of changes in mean temperatures versus temperature gradients in the recent widening of the Hadley circulation. *Journal of Climate*, **27**, 7450–7461, doi:10.1175/JCLI-D-14-00140.1.
- [3] Albani, S. and N. M. Mahowald, 2019: Paleodust insights into dust impacts on climate. *Journal of Climate*, **32**, no. 22, 7897–7913, doi:10.1175/JCLI-D-18-0742.1.
- [4] Alfaro-Sánchez, R., H. Nguyen, S. Klesse, A. Hudson, S. Belmecheri, N. Köse, H. Díaz, R. Monson, R. Villalba, and V. Trouet, 2018: Climatic and volcanic forcing of tropical belt northern boundary over the past 800 years. *Nature Geoscience*, **11**, no. 12, 933–938, doi:10.1038/s41561-018-0242-1.
- [5] Allen, R., S. Sherwood, J. Norris, and C. Zender, 2012: The equilibrium response to idealized thermal forcings in a comprehensive GCM: Implications for recent tropical expansion. *Atmospheric Chemistry and Physics*, **12**, no. 10, 4795–4816, doi:10.5194/acp-12-4795-2012.
- [6] Allen, R. J. and O. Ajoku, 2016: Future aerosol reductions and widening of the northern tropical belt. *Journal of Geophysical Research: Atmospheres*, **121**, no. 12, 6765–6786, doi:10.1002/2016JD024803.

- [7] Allen, R. J. and M. Kovilakam, 2017: The role of natural climate variability in recent tropical expansion. *Journal of Climate*, **30**, no. 16, 6329–6350, doi:10.1175/JCLI-D-16-0735.1.
- [8] Allen, R. J., S. C. Sherwood, J. R. Norris, and C. S. Zender, 2012: Recent Northern Hemisphere tropical expansion primarily driven by black carbon and tropospheric ozone. *Nature*, **485**, no. 7398, 350–354, doi:10.1038/nature11097.
- [9] Armour, K. C., N. Siler, A. Donohoe, and G. H. Roe, 2019: Meridional atmospheric heat transport constrained by energetics and mediated by large-scale diffusion. *Journal of Climate*, **32**, no. 12, 3655–3680.
- [10] Baldassare, D., T. Reichler, P. Plink-Björklund, and J. Slawson, 2023: Large uncertainty in observed estimates of tropical width from the meridional stream function. *Weather and Climate Dynamics*, **4**, no. 2, 531–541.
- [11] Banerjee, A., J. C. Fyfe, L. M. Polvani, D. Waugh, and K.-L. Chang, 2020: A pause in Southern Hemisphere circulation trends due to the Montreal Protocol. *Nature*, **579**, no. 7800, 544–548.
- [12] Bangalath, H. K. and G. Stenchikov, 2015: Role of dust direct radiative effect on the tropical rain belt over Middle East and North Africa: A high-resolution AGCM study. *Journal of Geophysical Research: Atmospheres*, **120**, no. 10, 4564–4584, doi:10.1002/2015JD023122.
- [13] Becker, E., G. Schmitz, and R. Geprägs, 1997: The feedback of midlatitude waves onto the Hadley cell in a simple general circulation model. *Tellus*, **49A**, 182–199, doi:10.1034/j.1600-0870.1997.t01-1-00003.x.
- [14] Berger, A., 1988: Milankovitch theory and climate. *Reviews of Geophysics*, **26**, no. 4, 624–657, doi:10.1029/RG026i004p00624.
- [15] Birner, T., S. M. Davis, and D. J. Seidel, 2014: The changing width of earth's tropical belt. *Physics Today*, **67**, no. 12, 38–44.
- [16] Bjerknes, J., 1966: A possible response of the atmospheric Hadley circulation to equatorial anomalies of ocean temperature. *Tellus*, **18**, no. 4, 820–829, doi:10.1111/j.2153-3490.1966.tb00303.x.
- [17] Boos, W. R. and K. A. Emanuel, 2008: Wind–evaporation feedback and abrupt seasonal transitions of weak, axisymmetric Hadley circulations. *Journal of the Atmospheric Sciences*, **65**, 2194–2214, doi:10.1175/2007JAS2608.1.
- [18] Bordoni, S. and T. Schneider, 2008: Monsoons as eddy-mediated regime transitions of the tropical overturning circulation. *Nature Geoscience*, **1**, 515–519, doi:10.1038/ngeo248.
- [19] — 2010: Regime transitions of steady and time-dependent Hadley circulations: Comparison of axisymmetric and eddy-permitting simulations. *Journal of the Atmospheric Sciences*, **67**, 1643–1654, doi:10.1175/2009JAS3294.1.
- [20] Broccoli, A. J., K. A. Dahl, and R. J. Stouffer, 2006: Response of the ITCZ to northern hemisphere cooling. *Geophysical Research Letters*, **33**, L01702, doi:10.1029/2005GL024546.
- [21] Bryson, R. A., 1974: A perspective on climatic change. *Science*, **184**, no. 4138, 753–760, doi:10.1126/science.184.4138.753.  
URL <http://www.jstor.org/stable/1738645>
- [22] Burls, N. J., R. C. Blamey, B. A. Cash, E. T. Swenson, A. al Fahad, M.-J. M. Bopape, D. M. Straus, and C. J. Reason, 2019: The Cape Town “Day Zero” drought and Hadley cell expansion. *Nature Partner Journals Climate and Atmospheric Science*, **2**, no. 1, 1–8, doi:10.1038/s41612-019-0084-6.
- [23] Caballero, R., 2007: Role of eddies in the interannual variability of Hadley cell strength. *Geophys. Res. Lett.*, **34**, L22705, doi:10.1029/2007GL030971.
- [24] — 2008: Hadley cell bias in climate models linked to extratropical eddy stress. *Geophysical Research Letters*, **35**, L18709, doi:10.1029/2008GL035084.

- [25] Caballero, R., R. T. Pierrehumbert, and J. L. Mitchell, 2008: Axisymmetric, nearly inviscid circulations in non-condensing radiative-convective atmospheres. *Quarterly Journal of the Royal Meteorological Society*, **134**, 1269–1285, doi:10.1002/qj.271.
- [26] Ceppi, P. and D. L. Hartmann, 2013: On the speed of the eddy-driven jet and the width of the Hadley cell in the Southern Hemisphere. *Journal of Climate*, **26**, 3450–3465, doi:10.1175/JCLI-D-12-00414.1.
- [27] Charlson, R. J., J. Langner, H. Rodhe, C. Leovy, and S. Warren, 1991: Perturbation of the northern hemisphere radiative balance by backscattering from anthropogenic sulfate aerosols. *Tellus A: Dynamic Meteorology and Oceanography*, **43**, no. 4, 152–163.
- [28] Charlson, R. J., S. Schwartz, J. Hales, R. D. Cess, J. J. Coakley, J. Hansen, and D. Hofmann, 1992: Climate forcing by anthropogenic aerosols. *Science*, **255**, no. 5043, 423–430.
- [29] Charney, J. G., 1975: Dynamics of deserts and drought in the sahel. *Quarterly Journal of the Royal Meteorological Society*, **101**, no. 428, 193–202, doi:10.1002/qj.49710142802.
- [30] Chemke, R. and L. Polvani, 2021: Elucidating the mechanisms responsible for Hadley cell weakening under  $4\times$   $\text{CO}_2$  forcing. *Geophysical Research Letters*, **48**, no. 3, e2020GL090348, doi:10.1029/2020GL090348.
- [31] Chemke, R., L. Polvani, and C. Deser, 2019: The effect of arctic sea ice loss on the hadley circulation. *Geophysical Research Letters*, **46**, no. 2, 963–972, doi:10.1029/2018GL081110.
- [32] Chemke, R. and L. M. Polvani, 2019: Exploiting the abrupt  $4\times$   $\text{CO}_2$  scenario to elucidate tropical expansion mechanisms. *Journal of Climate*, **32**, no. 3, 859–875, doi:10.1175/JCLI-D-18-0330.1.
- [33] — 2019: Opposite tropical circulation trends in climate models and in reanalyses. *Nature Geoscience*, **12**, no. 7, 528–532.
- [34] Chemke, R. and J. Yuval, 2023: Human-induced weakening of the northern hemisphere tropical circulation. *Nature*, 1–4, doi:10.1038/s41586-023-05903-1.
- [35] Chen, J. and S. Bordoni, 2014: Orographic effects of the Tibetan Plateau on the East Asian summer monsoon: An energetic perspective. *Journal of Climate*, **27**, no. 8, 3052–3072, doi:10.1175/JCLI-D-13-00479.1.
- [36] Chen, K., S. and Wei, W. Chen, , and L. Song, 2014: Regional changes in the annual mean Hadley circulation in recent decades. *Journal of Geophysical Research: Atmospheres*, **119**, 7815–7832, doi:10.1002/2014JD021540.
- [37] Cheng, W., D. G. MacMartin, B. Kravitz, D. Visoni, E. M. Bednarz, Y. Xu, Y. Luo, L. Huang, Y. Hu, P. W. Staten, et al., 2022: Changes in hadley circulation and intertropical convergence zone under strategic stratospheric aerosol geoengineering. *npj Climate and Atmospheric Science*, **5**, no. 1, 1–11, doi:10.1038/s41612-022-00254-6.
- [38] Choi, J., S.-W. Son, and R. J. Park, 2019: Aerosol versus greenhouse gas impacts on southern hemisphere general circulation changes. *Climate Dynamics*, **52**, 4127–4142.
- [39] Chou, C. and C.-A. Chen, 2010: Depth of convection and the weakening of tropical circulation in global warming. *Journal of Climate*, **23**, 3019–3030, doi:10.1175/2010JCLI3383.1.
- [40] Chou, C. and J. D. Neelin, 2004: Mechanisms of global warming impacts on regional tropical precipitation. *Journal of Climate*, **17**, 2688–2701, doi:10.1175/1520-0442(2004)017<2688:MOGWIO>2.0.CO;2.
- [41] Chou, C., T.-C. Wu, and P.-H. Tan, 2013: Changes in gross moist stability in the tropics under global warming. *Climate Dynamics*, **41**, 2481–2496, doi:10.1007/s00382-013-1703-2.
- [42] Colose, C. M., A. N. LeGrande, and M. Vuille, 2016: Hemispherically asymmetric volcanic forcing of tropical hydroclimate during the last millennium. *Earth System Dynamics*, **7**, no. 3, 681–696, doi:10.5194/esd-7-681-2016.

- [43] Cook, K. H., 2003: Role of continents in driving the Hadley cells. *Journal of the atmospheric sciences*, **60**, no. 7, 957–976, doi:10.1175/1520-0469(2003)060<0957:ROCIDT>2.0.CO;2.
- [44] Craig, P. M., D. Ferreira, and J. Methven, 2020: Monsoon-induced zonal asymmetries in moisture transport cause anomalous Pacific precipitation minus evaporation. *Geophysical Research Letters*, **47**, no. 18, e2020GL088659, doi:10.1029/2020GL088659.
- [45] Czaja, A. and J. C. Marshall, 2006: The partitioning of poleward heat transport between the atmosphere and ocean. *Journal of Atmospheric Sciences*, **63**, 1498–1511.
- [46] D'Agostino, R., J. Bader, S. Bordoni, D. Ferreira, and J. Jungclaus, 2019: Northern Hemisphere monsoon response to mid-Holocene orbital forcing and greenhouse gas-induced global warming. *Geophysical Research Letters*, **46**, no. 3, 1591–1601, doi:10.1029/2018GL081589.
- [47] D'Agostino, R., J. R. Brown, A. Moise, H. Nguyen, P. L. S. Dias, and J. Jungclaus, 2020: Contrasting southern hemisphere monsoon response: MidHolocene orbital forcing versus future greenhouse gas-induced global warming. *Journal of Climate*, **33**, no. 22, 9595–9613, doi:10.1175/JCLI-D-19-0672.1.
- [48] D'Agostino, R. and P. Lionello, 2017: Evidence of global warming impact on the evolution of the Hadley circulation in ecmwf centennial reanalyses. *Climate Dynamics*, **48**, no. 9–10, 3047–3060, doi:10.1007/s00382-016-3250-0.
- [49] D'Agostino, R., P. Lionello, O. Adam, and T. Schneider, 2017: Factors controlling Hadley circulation changes from the Last Glacial Maximum to the end of the 21st century. *Geophysical Research Letters*, **44**, no. 16, 8585–8591, doi:10.1002/2017GL074533.
- [50] D'Agostino, R., A. L. Scambiati, J. Jungclaus, and P. Lionello, 2020: Poleward shift of northern subtropics in winter: Time of emergence of zonal versus regional signals. *Geophysical Research Letters*, **47**, no. e2020GL089325, doi:10.1029/2020GL089325.
- [51] D'Agostino, R. and C. Timmreck, 2022: Sensitivity of regional monsoons to idealised equatorial volcanic eruption of different sulfur emission strengths. *Environmental Research Letters*, **17**, no. 5, 054001, doi:10.1088/1748-9326/ac62af.
- [52] Davis, N. and T. Birner, 2016: Climate model biases in the width of the tropical belt. *Journal of Climate*, **29**, no. 5, 1935–1954, doi:10.1175/JCLI-D-15-0336.1.
- [53] — 2017: On the discrepancies in tropical belt expansion between reanalyses and climate models and among tropical belt width metrics. *Journal of Climate*, **30**, no. 4, 1211–1231.
- [54] Davis, N. A. and T. Birner, 2019: Eddy influences on the Hadley circulation. *J. Adv. Model. Earth Syst.*, **11**, 1563–1581, doi:10.1029/2018MS001554.
- [55] — 2021: Eddy-mediated Hadley cell expansion due to axisymmetric angular momentum adjustment to greenhouse gas forcings. *J. Atmos. Sci.*, doi:10.1175/JAS-D-20-0149.1.
- [56] Davis, N. A. and S. M. Davis, 2018: Reconciling Hadley cell expansion trend estimates in reanalyses. *Geophysical Research Letters*, **45**, no. 20, 11–439, doi:10.1029/2018GL079593.
- [57] Davis, S. M. and K. H. Rosenlof, 2012: A multidagnostic intercomparison of tropical-width time series using reanalyses and satellite observations. *Journal of Climate*, **25**, no. 4, 1061–1078, doi:10.1175/JCLI-D-11-00127.1.
- [58] Dee, D. P., S. M. Uppala, A. J. Simmons, P. Berrisford, P. Poli, S. Kobayashi, U. Andrae, M. Balmaseda, G. Balsamo, d. P. Bauer, et al., 2011: The era-interim reanalysis: Configuration and performance of the data assimilation system. *Quarterly Journal of the royal meteorological society*, **137**, no. 656, 553–597.
- [59] Diaz, H. F. and R. S. Bradley, 2004: The hadley circulation: present, past, and future. *The Hadley Circulation: Present, Past and Future*, Springer, 1–5.

- [60] Dima, I. M. and J. M. Wallace, 2003: On the seasonality of the Hadley cell. *J. Atmos. Sci.*, **60**, 1522–1527, doi:10.1175/1520-0469(2003)060<1522:OTSOTH>2.0.CO;2.
- [61] Dogar, M. M., 2018: Impact of tropical volcanic eruptions on Hadley circulation using a high-resolution AGCM. *Current Science*, doi:10.18520/cs/v114/i06/1284-1294.
- [62] Dogar, M. M. and T. Sato, 2019: Regional Climate Response of Middle Eastern, African, and South Asian Monsoon Regions to Explosive Volcanism and ENSO Forcing. *Journal of Geophysical Research: Atmospheres*, **124**, no. 14, 7580–7598, doi:10.1029/2019JD030358.
- [63] Donohoe, A., J. Marshall, D. Ferreira, and D. McGee, 2013: The relationship between ITCZ location and cross equatorial atmospheric heat transport; from the seasonal cycle to the Last Glacial Maximum. *Journal of Climate*, **26**, 3597–3618, doi:10.1175/JCLI-D-12-00467.1.
- [64] Dunning, C. M., E. Black, and R. P. Allan, 2018: Later wet seasons with more intense rainfall over Africa under future climate change. *Journal of Climate*, **31**, 9719–9738, doi:10.1175/JCLI-D-18-0102.1.
- [65] Eliassen, A., 1951: Slow thermally or frictionally controlled meridional circulation in a circular vortex. *Astrophysica Norvegica*, **5**, 19.
- [66] Fang, M. and K. K. Tung, 1996: A simple model of nonlinear Hadley circulation with an ITCZ: Analytic and numerical solutions. *J. Atmos. Sci.*, **53**, 1241–1261, doi:10.1175/1520-0469(1996)053<1241:ASMONH>2.0.CO;2.
- [67] — 1999: Time-dependent nonlinear Hadley circulation. *J. Atmos. Sci.*, **56**, 1797–1807, doi:10.1175/1520-0469(1999)056<1797:TDNHC>2.0.CO;2.
- [68] Faulk, S., J. Mitchell, and S. Bordoni, 2017: Effects of rotation rate and seasonal forcing on the ITCZ extent in planetary atmospheres. *J. Atmos. Sci.*, **74**, 665–678, doi:10.1175/JAS-D-16-0014.1.
- [69] Ferreira, D., P. Cessi, H. K. Coxall, A. de Boer, H. A. Dijkstra, S. S. Drijfhout, T. Eldevik, N. Harnik, J. F. McManus, D. P. Marshall, J. Nilsson, F. Roquet, T. Schneider, and R. C. Wills, 2018: Atlantic-Pacific Asymmetry in Deep-Water Formation. *Annu. Rev. Earth Planet. Sci.*, **46**, doi:10.1146/annurev-earth-082517-010045.
- [70] Ferreira, D., J. Marshall, T. Ito, and D. McGee, 2018: Linking glacial-interglacial states to multiple equilibria of climate. *Geophysical Research Letters*, **45**, no. 17, 9160–9170, doi:10.1029/2018GL077019.
- [71] Fontaine, B., P. Roucou, M. Gaetani, and R. Marteau, 2011: Recent changes in precipitation, ITCZ convection and northern tropical circulation over North Africa (1979–2007). *International Journal of Climatology*, **31**, no. 5, 633–648, doi:10.1002/joc.2108.
- [72] Forget, G. and D. Ferreira, 2019: Global ocean heat transport dominated by heat export from the tropical Pacific. *Nature Geoscience*, **12**, 351–354, doi:10.1038/s41561-019-0333-7.
- [73] Frierson, D. M. and Y.-T. Hwang, 2012: Extratropical influence on itcz shifts in slab ocean simulations of global warming. *Journal of Climate*, **25**, no. 2, 720–733, doi:10.1175/JCLI-D-11-00116.1.
- [74] Frierson, D. M., Y.-T. Hwang, N. S. Fučkar, R. Seager, S. M. Kang, A. Donohoe, E. A. Maroon, X. Liu, and D. S. Battisti, 2013: Contribution of ocean overturning circulation to tropical rainfall peak in the Northern hemisphere. *Nature Geoscience*, **6**, no. 11, 940–944, doi:10.1038/ngeo1987.
- [75] Frierson, D. M., J. Lu, and G. Chen, 2007: Width of the Hadley cell in simple and comprehensive general circulation models. *Geophysical Research Letters*, **34**, no. 18, doi:10.1029/2007GL031115.
- [76] Gadgil, S., 2018: The monsoon system: Land-sea breeze or the ITCZ? *Journal of Earth System Science*, **127**, 1, doi:10.1007/s12040-017-0916-x.

- [77] Galanti, E., D. Raiter, Y. Kaspi, and E. Tziperman, 2022: Spatial patterns of the tropical meridional circulation: drivers and teleconnections. *Journal of Geophysical Research: Atmospheres*, **127**, no. 2, e2021JD035531, doi:10.1029/2021JD035531.
- [78] Ganopolski, A. and V. Brovkin, 2017: Simulation of climate, ice sheets and co<sub>2</sub> evolution during the last four glacial cycles with an earth system model of intermediate complexity. *Climate of the Past*, **13**, no. 12, 1695–1716, doi:10.5194/cp-13-1695-2017.
- [79] Garfinkel, C. I., D. W. Waugh, and L. M. Polvani, 2015: Recent hadley cell expansion: The role of internal atmospheric variability in reconciling modeled and observed trends. *Geophysical Research Letters*, **42**, no. 24, 10–824.
- [80] Geen, R., S. Bordon, D. S. Battisti, and K. L. Hui, 2021: Monsoons, ITCZs and the Concept of the Global Monsoon. *Rev. Geophys.*, **in press**, doi:10.1029/2020RG000700.
- [81] Geen, R., F. H. Lambert, and G. K. Vallis, 2018: Regime change behavior during Asian monsoon onset. *J. Climate*, **31**, 3327–3348, doi:10.1175/JCLI-D-17-0118.1.
- [82] — 2019: Processes and Timescales in Onset and Withdrawal of “Aquaplanet Monsoons”. *Journal of the Atmospheric Sciences*, **76**, 2357–2373, doi:10.1175/JAS-D-18-0214.1.
- [83] Gerber, E. P. and S.-W. Son, 2014: Quantifying the summertime response of the austral jet stream and hadley cell to stratospheric ozone and greenhouse gases. *Journal of Climate*, **27**, no. 14, 5538–5559.
- [84] Graversen, R. and M. Burtu, 2016: Arctic amplification enhanced by latent energy transport of atmospheric planetary waves. *Quart. J. Roy. Meteor. Soc.*, **142**, no. 698, 2046–2054.
- [85] Green, B., J. Marshall, and J.-M. Campin, 2019: The ‘sticky’ ITCZ: ocean-moderated ITCZ shifts. *Climate dynamics*, **53**, no. 1, 1–19, doi:10.1007/s00382-019-04623-5.
- [86] Griffiths, P. T., L. T. Murray, G. Zeng, Y. M. Shin, N. L. Abraham, A. T. Archibald, M. Deushi, L. K. Emmons, I. E. Galbally, B. Hassler, et al., 2021: Tropospheric ozone in CMIP6 simulations. *Atmospheric Chemistry and Physics*, **21**, no. 5, 4187–4218, doi:10.5194/acp-21-4187-2021.
- [87] Grise, K. M. and S. M. Davis, 2020: Hadley cell expansion in CMIP6 models. *Atmospheric Chemistry and Physics*, **20**, no. 9, 5249–5268, doi:10.5194/acp-20-5249-2020.
- [88] Grise, K. M., S. M. Davis, I. R. Simpson, D. W. Waugh, Q. Fu, R. J. Allen, K. H. Rosenlof, C. C. Ummenhofer, K. B. Karnauskas, A. C. Maycock, et al., 2019: Recent tropical expansion: natural variability or forced response? *Journal of Climate*, **32**, no. 5, 1551–1571, doi:10.1175/JCLI-D-18-0444.1.
- [89] Grise, K. M., S. M. Davis, P. W. Staten, and O. Adam, 2018: Regional and seasonal characteristics of the recent expansion of the tropics. *Journal of Climate*, **31**, no. 17, 6839–6856, doi:10.1175/JCLI-D-18-0060.1.
- [90] Guendelman, I. and Y. Kaspi, 2018: An axisymmetric limit for the width of the Hadley cell on planets with large obliquity and long seasonality. *Geophys. Res. Lett.*, **45**, 13–213, doi:10.1029/2018GL080752.
- [91] Hadley, G., 1735: VI. concerning the cause of the general trade-winds. *Philosophical Transactions of the Royal Society of London*, **39**, no. 437, 58–62, doi:10.1098/rstl.1735.0014.
- [92] Halley, E., 1687: An historical account of the trade winds, and monsoons, observable in the seas between and near the Tropicks, with an attempt to assign the physical cause of the said winds. *Philosophical Transactions of the Royal Society of London*, **16**, no. 183, 153–168, doi:10.1098/rstl.1686.0026.  
URL <https://royalsocietypublishing.org/doi/abs/10.1098/rstl.1686.0026>
- [93] Hays, J. D., J. Imbrie, N. J. Shackleton, et al., 1976: Variations in the Earth's orbit: pacemaker of the ice ages. *science*, **194**, no. 4270, 1121–1132, doi:10.1126/science.194.4270.1121.



- [94] Haywood, J. M., A. Jones, N. Bellouin, and D. Stephenson, 2013: Asymmetric forcing from stratospheric aerosols impacts Sahelian rainfall. *Nature Climate Change*, **3**, no. 7, 660–665, doi:10.1038/nclimate1857.
- [95] Held, I., 2001: The partitioning of the poleward energy transport between the tropical ocean and atmosphere. *Journal of Atmospheric Sciences*, **58**, 943–948, doi:10.1175/1520-0469(2001)058<0943:TPOTPE>2.0.CO;2.
- [96] Held, I. M., 2000: The general circulation of the atmosphere. *Proc. Geophysical Fluid Dynamics Program*, Woods Hole Oceanographic Institution, 1–54.  
URL <https://www.whoi.edu/fileserver.do?id=21464&pt=10&p=17332>
- [97] Held, I. M. and A. Y. Hou, 1980: Nonlinear Axially Symmetric Circulations in a Nearly Inviscid Atmosphere. *J. Atmos. Sci.*, **37**, 515–533, doi:10.1175/1520-0469(1980)037<0515:NASCIA>2.0.CO;2.
- [98] Held, I. M. and B. J. Soden, 2006: Robust responses of the hydrological cycle to global warming. *Journal of climate*, **19**, no. 21, 5686–5699, doi:10.1175/JCLI3990.1.
- [99] Hersbach, H., B. Bell, P. Berrisford, S. Hirahara, A. Horányi, J. Muñoz-Sabater, J. Nicolas, C. Peubey, R. Radu, D. Schepers, et al., 2020: The ERA5 global reanalysis. *Quarterly Journal of the Royal Meteorological Society*, **146**, no. 730, 1999–2049, doi:10.1002/qj.3803.
- [100] Hildebrandsson, H. H. and L. P. T. de Bort, 1900: *Les bases de la météorologie dynamique: historique-état de nos connaissances*, volume 2. Gauthier-Villars et fils.
- [101] Hill, S. A., S. Bordoni, and J. L. Mitchell, 2019: Axisymmetric constraints on cross-equatorial Hadley cell extent. *J. Atmos. Sci.*, **76**, 1547–1564, doi:10.1175/JAS-D-18-0306.1.
- [102] — 2022: A theory for the Hadley cell descending and ascending edges throughout the annual cycle. *Journal of the Atmospheric Sciences*, **79**, no. 10, 2515–2528, doi:10.1175/JAS-D-21-0328.1.
- [103] Hill, S. A., Y. Ming, and I. M. Held, 2015: Mechanisms of forced tropical meridional energy flux change. *Journal of Climate*, **28**, no. 5, 1725 – 1742, doi:10.1175/JCLI-D-14-00165.1.
- [104] Hoskins, B. and G.-Y. Yang, 2021: The detailed dynamics of the hadley cell. part ii: December–february. *Journal of Climate*, **34**, no. 2, 805–823.
- [105] Hoskins, B., G.-Y. Yang, and R. Fonseca, 2020: The detailed dynamics of the june–august hadley cell. *Quarterly Journal of the Royal Meteorological Society*, **146**, no. 727, 557–575.
- [106] Hoskins, B. J. and G. Yang, 2021: The detailed dynamics of the Hadley Cell. Part 2: December to February. *Journal of Climate*, **34**, no. 2, 805–823.  
URL <https://doi.org/10.1175/JCLI-D-20-0504.1>
- [107] Hoskins, B. J., G. Yang, and R. M. Fonseca, 2020: The detailed dynamics of the June–August Hadley Cell. *Q J R Meteorol Soc.*, **146**, 557–575.  
URL <https://doi.org/10.1002/qj.3702>
- [108] Hou, A. Y., 1998: Hadley circulation as a modulator of the extratropical climate. *Journal of the atmospheric sciences*, **55**, no. 14, 2437–2457, doi:10.1175/1520-0469(1998)055<2437:HCAAMO>2.0.CO;2.
- [109] Hu, D., Z. Guan, and W. Tian, 2019: Signatures of the arctic stratospheric ozone in northern hadley circulation extent and subtropical precipitation. *Geophysical Research Letters*, **46**, no. 21, 12340–12349, doi:10.1029/2019GL085292.
- [110] Hu, Y. and Q. Fu, 2007: Observed poleward expansion of the Hadley circulation since 1979. *Atmospheric Chemistry and Physics*, **7**, no. 19, 5229–5236, doi:10.5194/acp-7-5229-2007.
- [111] Hu, Y., H. Huang, and C. Zhou, 2018: Widening and weakening of the hadley circulation under global warming. *Science Bulletin*, **63**, no. 10, 640–644.

- [112] Hu, Y. and C. Zhou, 2010: Decadal changes in the Hadley circulation. *Advances in Geosciences*, **16**, 61.
- [113] Hu, Y., C. Zhou, and J. Liu, 2011: Observational evidence for poleward expansion of the hadley circulation. *Advances in Atmospheric Sciences*, **28**, no. 1, 33–44.
- [114] Iles, C. E. and G. C. Hegerl, 2014: The global precipitation response to volcanic eruptions in the CMIP5 models. *Environmental Research Letters*, **9**, no. 10, 104012, doi:10.1088/1748-9326/9/10/104012.
- [115] — 2015: Systematic change in global patterns of streamflow following volcanic eruptions. *Nature geoscience*, **8**, no. 11, 838–842, doi:10.1038/ngeo2545.
- [116] Imbrie, J. and J. Z. Imbrie, 1980: Modeling the climatic response to orbital variations. *Science*, **207**, no. 4434, 943–953, doi:10.1126/science.207.4434.943.
- [117] Inoue, K. and L. E. Back, 2017: Gross moist stability analysis: Assessment of satellite-based products in the gms plane. *Journal of the Atmospheric Sciences*, **74**, no. 6, 1819–1837.
- [118] Jaliha, C., J. Srinivasan, and A. Chakraborty, 2019: Modulation of Indian monsoon by water vapor and cloud feedback over the past 22,000 years. *Nature communications*, **10**, no. 1, 1–8, doi:10.1038/s41467-019-13754-6.
- [119] Johanson, C. M. and Q. Fu, 2009: Hadley cell widening: Model simulations versus observations. *Journal of Climate*, **22**, no. 10, 2713–2725, doi:10.1175/2008JCLI2620.1.
- [120] Kang, S. M., C. Deser, and L. M. Polvani, 2013: Uncertainty in climate change projections of the hadley circulation: The role of internal variability. *Journal of Climate*, **26**, no. 19, 7541–7554.
- [121] Kang, S. M., I. M. Held, D. M. Frierson, and M. Zhao, 2008: The response of the itcz to extratropical thermal forcing: Idealized slab-ocean experiments with a gcm. *Journal of Climate*, **21**, no. 14, 3521–3532.
- [122] Kang, S. M., I. M. Held, and S. Xie, 2014: Contrasting the tropical responses to zonally asymmetric extratropical and tropical thermal forcing. *Climate Dynamics*, **42**, 2033–2043, doi:10.1007/s00382-013-1863-0.
- [123] Kang, S. M., L. Polvani, J. Fyfe, and M. Sigmond, 2011: Impact of polar ozone depletion on subtropical precipitation. *Science*, **332**, no. 6032, 951–954, doi:10.1126/science.1202131.
- [124] Kang, S. M. and L. M. Polvani, 2011: The interannual relationship between the latitude of the eddy-driven jet and the edge of the Hadley cell. *J. Climate*, **24**, 563–568, doi:10.1175/2010JCLI4077.1.
- [125] Karnauskas, K. B. and C. C. Ummenhofer, 2014: On the dynamics of the Hadley circulation and subtropical drying. *Climate Dynamics*, **42**, 2259–2269.  
URL <https://doi.org/10.1007/s00382-014-2129-1>
- [126] Kaufman, Y., D. Tanré, O. Dubovik, A. Karnieli, and L. Remer, 2001: Absorption of sunlight by dust as inferred from satellite and ground-based remote sensing. *Geophysical Research Letters*, **28**, no. 8, 1479–1482, doi:10.1029/2000GL012647.
- [127] Khon, V., W. Park, M. Latif, I. I. Mokhov, and B. Schneider, 2012: Tropical circulation and hydrological cycle response to orbital forcing. *Geophysical research letters*, **39**, no. 15, doi:10.1029/2012GL052482.
- [128] Kidston, J., C. W. Cairns, and P. Paga, 2013: Variability in the width of the tropics and the annular modes. *Geophys. Res. Lett.*, **40**, 2328–2332, doi:10.1029/2012GL054165.
- [129] Kim, H.-K. and S. Lee, 2001: Hadley cell dynamics in a primitive equation model. Part II: Nonaxisymmetric flow. *J. Atmos. Sci.*, **58**, 2859–2871, doi:10.1175/1520-0469(2001)058<2859:HCDIAP>2.0.CO;2.
- [130] Kim, Y. H., S. K. Min, S. W. Son, and J. Choi, 2017: Attribution of the local Hadley cell widening in the Southern Hemisphere. *Geophysical Research Letters*, **44**, 1015–1024.  
URL <https://doi.org/10.1002/2016GL072353>

- [131] Kuo, H. L., 1956: Forced and free meridional circulations in the atmosphere. *J. Meteorol.*, **13**, 561–568, doi:10.1175/1520-0469(1956)013<0561:FAFMCI>2.0.CO;2.
- [132] Lacis, A., J. Hansen, and M. Sato, 1992: Climate forcing by stratospheric aerosols. *Geophysical Research Letters*, **19**, no. 15, 1607–1610, doi:10.1029/92GL01620.
- [133] Lau, K., K. Kim, Y. Sud, and G. Walker, 2009: A GCM study of the response of the atmospheric water cycle of West Africa and the Atlantic to Saharan dust radiative forcing. *Annales Geophysicae*, Copernicus GmbH, volume 27, 4023–4037.
- [134] Lau, W. K. and K.-M. Kim, 2015: Robust hadley circulation changes and increasing global dryness due to co2 warming from cmip5 model projections. *Proceedings of the National Academy of Sciences*, **112**, 3630–3635.
- [135] Lau, W. K. and W. Tao, 2020: Precipitation–radiation–circulation feedback processes associated with structural changes of the itcz in a warming climate during 1980–2014: An observational portrayal. *Journal of Climate*, **33**, no. 20, 8737–8749.
- [136] Lembo, V., D. Folini, M. Wild, and P. Lionello, 2019: Inter-hemispheric differences in energy budgets and cross-equatorial transport anomalies during the 20th century. *Climate dynamics*, **53**, no. 1, 115–135, doi:10.1007/s00382-018-4572-x.
- [137] Levine, X. J. and T. Schneider, 2011: Response of the Hadley circulation to climate change in an aquaplanet GCM coupled to a simple representation of ocean heat transport. *J. Atmos. Sci.*, **68**, 769–783, doi:10.1175/2010JAS3553.1.
- [138] — 2015: Baroclinic eddies and the extent of the Hadley circulation: An idealized GCM study. *J. Atmos. Sci.*, **72**, 2744–2761, doi:10.1175/JAS-D-14-0152.1.
- [139] Liang, X.-Z. and W.-C. Wang, 1998: Associations between China monsoon rainfall and tropospheric jets. *Quarterly Journal of the Royal Meteorological Society*, **124**, no. 552, 2597–2623, doi:10.1002/qj.49712455204.
- [140] Lindzen, R. S. and A. V. Hou, 1988: Hadley circulations for zonally averaged heating centered off the equator. *Journal of the Atmospheric Sciences*, **45**, no. 17, 2416–2427, doi:10.1175/1520-0469(1988)045<2416:HCFZAH>2.0.CO;2.
- [141] Liu, C., R. P. Allan, M. Mayer, P. Hyder, D. Desbruyeres, L. Cheng, J. Xu, F. Xu, and Y. Zhang, 2020: Variability in the global energy budget and transports 1985–2017. *Climate Dynamics*, **55**, 3381–3396, doi:10.1007/s00382-020-05451-8.
- [142] Liu, F., J. Chai, B. Wang, J. Liu, X. Zhang, and Z. Wang, 2016: Global monsoon precipitation responses to large volcanic eruptions. *Scientific reports*, **6**, no. 1, 1–11, doi:10.1038/srep24331.
- [143] Liu, J., M. Song, Y. Hu, and X. Ren, 2012: Changes in the strength and width of the hadley circulation since 1871. *Climate of the Past*, **8**, no. 4, 1169–1175.
- [144] Lorenz, E. N., 1983: A history of prevailing ideas about the general circulation of the atmosphere. *Bulletin of the American Meteorological Society*, 730–734.
- [145] Lorenz, E. N. and F. N. Lorenz, 1967: *The nature and theory of the general circulation of the atmosphere*, volume 218. World Meteorological Organization Geneva.
- [146] Lu, J., G. Chen, and D. M. Frierson, 2008: Response of the zonal mean atmospheric circulation to El Niño versus global warming. *J. Climate*, **21**, 5835–5851, doi:10.1175/2008JCLI2200.1.
- [147] Lu, J., G. A. Vecchi, and T. Reichler, 2007: Expansion of the Hadley cell under global warming. *Geophysical Research Letters*, **34**, no. 6, doi:10.1029/2006GL028443.
- [148] Lucarini, V. and F. Ragone, 2011: Energetics of climate models: Net energy balance and meridional enthalpy transport. *Reviews of Geophysics*, **49**, no. 1, doi:10.1029/2009RG000323.

- [149] Lucas, C., B. Timbal, and H. Nguyen, 2014: The expanding tropics: A critical assessment of the observational and modeling studies. *Wiley Interdisciplinary Reviews: Climate Change*, **5**, no. 1, 89–112.
- [150] Luo, J.-J., W. Sasaki, and Y. Masumoto, 2012: Indian Ocean warming modulates Pacific climate change. *Proceedings of the National Academy of Sciences*, **109**, no. 46, 18701–18706, doi:10.1073/pnas.1210239109.
- [151] Ma, D., A. H. Sobel, Z. Kuang, M. S. Singh, and J. Nie, 2019: A moist entropy budget view of the South Asian summer monsoon onset. *Geophys. Res. Lett.*, **46**, 4476–4484, doi:10.1029/2019GL082089.
- [152] Ma, J., R. Chadwick, K.-H. Seo, C. Dong, G. Huang, G. R. Foltz, and J. H. Jiang, 2018: Responses of the tropical atmospheric circulation to climate change and connection to the hydrological cycle. *Annual Review of Earth and Planetary Sciences*, **46**, 549–580, doi:10.1146/annurev-earth-082517-010102.
- [153] Mamalakis, A., J. T. Randerson, J.-Y. Yu, M. S. Pritchard, G. Magnusdottir, P. Smyth, P. A. Levine, S. Yu, and E. Foufoula-Georgiou, 2021: Zonally contrasting shifts of the tropical rain belt in response to climate change. *Nature Climate Change*, doi:10.1038/s41558-020-00963-x.
- [154] Man, W., T. Zhou, and J. H. Jungclauss, 2014: Effects of large volcanic eruptions on global summer climate and East Asian monsoon changes during the last millennium: Analysis of MPI-ESM simulations. *Journal of Climate*, **27**, no. 19, 7394–7409, doi:10.1175/JCLI-D-13-00739.1.
- [155] Mantsis, D. F., S. Sherwood, R. Allen, and L. Shi, 2017: Natural variations of tropical width and recent trends. *Geophysical Research Letters*, **44**, no. 8, 3825–3832.
- [156] Marshall, J., A. Donohoe, D. Ferreira, and D. McGee, 2013: The ocean's role in setting the mean position of the atmosphere's ITCZ. *Climate Dynamics*, **42**, 1967–1979, doi:10.1007/s00382-013-1767-z.
- [157] McGee, D., A. Donohoe, J. Marshall, and D. Ferreira, 2014: Changes in ITCZ location and cross-equatorial heat transport at the Last Glacial Maximum, Heinrich Stadial 1, and the mid-Holocene. *Earth and Planetary Science Letters*, **390**, 69–79, doi:10.1002/2014GL062512.
- [158] McGee, D., E. Moreno-Chamarro, B. Green, J. Marshall, E. Galbraith, and L. Bradtmiller, 2018: Hemispherically asymmetric trade wind changes as signatures of past ITCZ shifts. *Quaternary Science Reviews*, **180**, 214–228, doi:10.1016/j.quascirev.2017.11.020.
- [159] McGregor, S., A. Timmermann, M. F. Stuecker, M. H. England, M. Merrifield, F.-F. Jin, and Y. Chikamoto, 2014: Recent Walker circulation strengthening and Pacific cooling amplified by Atlantic warming. *Nature Climate Change*, **4**, no. 10, 888–892, doi:10.1038/nclimate2330.
- [160] Milankovitch, M., 1941: Canon of insolation and the iceage problem. *Koniglich Serbische Akademie Beograd Special Publication*, **132**.
- [161] Miller, R. L., P. Knippertz, C. P. Garcia-Pando, J. P. Perlwitz, and I. Tegen, 2014: Impact of dust radiative forcing upon climate. *Mineral dust*, Springer, 327–357.
- [162] Min, S.-K. and S.-W. Son, 2013: Multimodel attribution of the Southern Hemisphere Hadley cell widening: Major role of ozone depletion. *Journal of Geophysical Research: Atmospheres*, **118**, no. 7, 3007–3015, doi:10.1002/jgrd.50232.
- [163] Mitas, C. M. and A. Clement, 2006: Recent behavior of the hadley cell and tropical thermodynamics in climate models and reanalyses. *Geophysical Research Letters*, **33**, no. 1.
- [164] Moon, H. and K.-J. Ha, 2020: Distinguishing changes in the Hadley circulation edge. *Theoretical and Applied Climatology*, **139**, no. 3, 1007–1017, doi:10.1007/s00704-019-03017-1.
- [165] Moreno-Chamarro, E., D. Ferreira, and J. Marshall, 2020: Polar phasing and cross-equatorial heat transfer following a simulated abrupt NH warming of a glacial climate. *Paleoceanography and Paleoclimatology*, **35**, e2019PA003810, doi:10.1029/2019PA003810.

- [166] Neelin, J. D. and I. M. Held, 1987: Modeling tropical convergence based on the moist static energy budget. *Monthly Weather Review*, **115**, no. 1, 3–12, doi:10.1175/1520-0493(1987)115<0003:MTCBOT>2.0.CO;2.
- [167] Nguyen, H., A. Evans, C. Lucas, I. Smith, and B. Timbal, 2013: The Hadley circulation in reanalyses: Climatology, variability, and change. *Journal of Climate*, **26**, no. 10, 3357–3376, doi:10.1175/JCLI-D-12-00224.1.
- [168] Nguyen, H., H. H. Hendon, E.-P. Lim, G. Bosch, E. Maloney, and B. Timbal, 2018: Variability of the extent of the Hadley circulation in the Southern Hemisphere: A regional perspective. *Climate Dynamics*, **50**, 129–142, doi:10.1007/s00382-017-3592-2.
- [169] Nguyen, H., C. Lucas, A. Evans, B. Timbal, and L. Hanson, 2015: Expansion of the southern hemisphere hadley cell in response to greenhouse gas forcing. *Journal of Climate*, **28**, 8067–8077, doi:10.1175/JCLI-D-15-0139.1.
- [170] Numaguti, A., 1993: Dynamics and energy balance of the Hadley circulation and the tropical precipitation zones: Significance of the distribution of evaporation. *Journal of the Atmospheric Sciences*, **50**, no. 13, 1874–1887, doi:10.1175/1520-0469(1993)050<1874:DAEBOT>2.0.CO;2.
- [171] Oort, A. H. and E. M. Rasmusson, 1970: On the annual variation of the monthly mean meridional circulation. *Monthly Weather Review*, **98**, no. 6, 423–442, doi:10.1175/1520-0493(1970)098<0423:OTAVOT>2.3.CO;2.
- [172] Oort, A. H. and J. J. Yienger, 1996: Observed interannual variability in the Hadley circulation and its connection to ENSO. *Journal of Climate*, **9**, no. 11, 2751–2767, doi:10.1175/1520-0442(1996)009<2751:OIVITH>2.0.CO;2.
- [173] Otto-Bliesner, B. L. and A. Clement, 2004: The sensitivity of the Hadley circulation to past and future forcings in two climate models. *The Hadley circulation: Present, past and future*, H. F. Diaz and R. S. Bradley, Eds., Springer, 437–464.
- [174] Paillard, D. and F. Parrenin, 2004: The Antarctic ice sheet and the triggering of deglaciations. *Earth and Planetary Science Letters*, **227**, no. 3–4, 263–271, doi:10.1016/j.epsl.2004.08.023.
- [175] Palmén, E. and L. A. Vuorela, 1963: On the mean meridional circulations in the northern hemisphere during the winter season. *Quarterly Journal of the Royal Meteorological Society*, **89**, no. 379, 131–138, doi:10.1002/qj.49708937910.
- [176] Pascale, S., L. M. V. Carvalho, D. K. Adams, C. L. Castro, and I. F. A. Cavalcanti, 2019: Current and future variations of the monsoons of the Americas in a warming climate. *Current Climate Change Reports*, **5**, 125–144, doi:10.1007/s40641-019-00135-w.
- [177] Pausata, F. S. R., L. Chafik, R. Caballero, and D. S. Battisti, 2015: Impacts of high-latitude volcanic eruptions on ENSO and AMOC. *Proceedings of the National Academy of Sciences of the USA*, **112**, no. 45, 13784–13788, doi:10.1073/pnas.1509153112.
- [178] Pausata, F. S. R., G. Messori, and Q. Zhang, 2016: Impacts of dust reduction on the northward expansion of the African monsoon during the Green Sahara period. *Earth and Planetary Science Letters*, **434**, 298–307, doi:10.1016/j.epsl.2015.11.049.
- [179] Pausata, F. S. R., D. Zanchettin, C. Karamperidou, R. Caballero, and D. S. Battisti, 2020: ITCZ shift and extratropical teleconnections drive ENSO response to volcanic eruptions. *Science Advances*, **6**, no. 23, eaaz5006, doi:10.1126/sciadv.aaz5006.
- [180] Peixoto, J. and A. Oort, 1992: *Physics of Climate*. American Institute of Physics.  
URL <https://books.google.co.uk/books?id=3tjKa0YzFRMC>
- [181] Philander, S. G. H., D. Gu, G. Lambert, T. Li., D. Halpern, N.-C. Lau, and R. C. Pacanowski, 1996: Why the ITCZ is Mostly north of the Equator. *Journal of Climate*, **9**, no. 12, 2958–2972, doi:10.1175/1520-0442(1996)009<2958:WTIIMN>2.0.CO;2.

- [182] Plumb, R. A. and A. Y. Hou, 1992: The response of a zonally symmetric atmosphere to subtropical thermal forcing: threshold behavior. *Journal of the Atmospheric Sciences*, **49**, no. 19, 1790–1799, doi:10.1175/1520-0469(1992)049<1790:TROAZS>2.0.CO;2.
- [183] Polvani, L. M., M. Previdi, and C. Deser, 2011: Large cancellation, due to ozone recovery, of future Southern Hemisphere atmospheric circulation trends. *Geophysical Research Letters*, **38**, no. 4, L04707, doi:10.1029/2011GL046712.
- [184] Polvani, L. M., D. W. Waugh, G. J. P. Correa, and S.-W. Son, 2011: Stratospheric ozone depletion: The main driver of twentieth-century atmospheric circulation changes in the Southern Hemisphere. *Journal of Climate*, **24**, no. 3, 795–812, doi:10.1175/2010JCLI3772.1.
- [185] Previdi, M. and B. G. Liepert, 2007: Annular modes and Hadley cell expansion under global warming. *Geophysical Research Letters*, **34**, no. 22, L22701, doi:10.1029/2007GL031243.
- [186] Previdi, M. and L. M. Polvani, 2014: Climate system response to stratospheric ozone depletion and recovery. *Quarterly Journal of the Royal Meteorological Society*, **140**, no. 685, 2401–2419, doi:10.1002/qj.2330.
- [187] Qiao, Y., W. Huang, and M. Jian, 2012: Impacts of El Niño–Southern Oscillation and local sea surface temperature on moisture source in Asian–Australian monsoon region in Boreal summer. *Aquatic Ecosystem Health & Management*, **15**, 31–38, doi:10.1080/14634988.2012.649667.
- [188] Quan, X.-W., H. F. Diaz, and M. P. Hoerling, 2004: Change in the tropical Hadley cell since 1950. *The Hadley circulation: Present, past and future*, H. F. Diaz and R. S. Bradley, Eds., Springer, 85–120.
- [189] Ramanathan, V. and G. Carmichael, 2008: Global and regional climate changes due to black carbon. *Nature Geoscience*, **1**, 221–227, doi:10.1038/ngeo156.
- [190] Randel, W. J. and I. M. Held, 1991: Phase speed spectra of transient eddy fluxes and critical layer absorption. *Journal of the Atmospheric Sciences*, **48**, no. 5, 688–697, doi:10.1175/1520-0469(1991)048<0688:PSSOTE>2.0.CO;2.
- [191] Raymond, D. J., S. L. Sessions, A. H. Sobel, and Ž. Fuchs, 2009: The mechanics of gross moist stability. *Journal of Advances in Modeling Earth Systems*, **1**, no. 3.
- [192] Rind, D. and J. Perlwitz, 2004: The response of the Hadley circulation to climate changes, past and future. *The Hadley circulation: Present, past and future*, H. F. Diaz and R. S. Bradley, Eds., Springer, 399–435.
- [193] Rodwell, M. J. and B. J. Hoskins, 1996: Monsoons and the dynamics of deserts. *Quarterly Journal of the Royal Meteorological Society*, **122**, no. 534, 1385–1404, doi:10.1002/qj.49712253408.
- [194] Rotstayn, L., M. A. Collier, S. J. Jeffrey, J. Kidston, J. Syktus, and K. Wong, 2013: Anthropogenic effects on the subtropical jet in the southern hemisphere: aerosols versus long-lived greenhouse gases. *Environmental Research Letters*, **8**, no. 1, 014030.
- [195] Satoh, M., 1994: Hadley circulations in radiative-convective equilibrium in an axially symmetric atmosphere. *Journal of the Atmospheric Sciences*, **51**, no. 13, 1947–1968, doi:10.1175/1520-0469(1994)051<1947:HCIREI>2.0.CO;2.
- [196] Satoh, M., M. Shiobara, and M. Takahashi, 1995: Hadley circulations and their rôles in the global angular momentum budget in two- and three-dimensional models. *Tellus*, **47**, no. 5, 548–560, doi:10.1034/j.1600-0870.1995.00104.x.
- [197] Scheff, J. and D. M. W. Frierson, 2012: Robust future precipitation declines in CMIP5 largely reflect the poleward expansion of model subtropical dry zones. *Geophysical Research Letters*, **39**, no. 18, L18704, doi:10.1029/2012GL052910.
- [198] Schneider, E. K., 1977: Axially symmetric steady-state models of the basic state for instability and climate studies. Part II. Nonlinear calculations. *Journal of the Atmospheric Sciences*, **34**, no. 2, 280–296, doi:10.1175/1520-0469(1977)034<0280:ASSSMO>2.0.CO;2.

- [199] Schneider, E. K. and R. S. Lindzen, 1977: Axially symmetric steady-state models of the basic state for instability and climate studies. Part I. Linearized calculations. *Journal of the Atmospheric Sciences*, **34**, no. 2, 263–279, doi:10.1175/1520-0469(1977)034<0263:ASSMO>2.0.CO;2.
- [200] Schneider, T., T. Bischoff, and G. H. Haug, 2014: Migrations and dynamics of the intertropical convergence zone. *Nature*, **513**, 45–53, doi:10.1038/nature13636.
- [201] Schneider, T. and S. Bordoni, 2008: Eddy-mediated regime transitions in the seasonal cycle of a Hadley circulation and implications for monsoon dynamics. *Journal of the Atmospheric Sciences*, **65**, no. 3, 915–934, doi:10.1175/2007JAS2415.1.
- [202] Schwendike, J., G. J. Berry, M. J. Reeder, C. Jakob, P. Govekar, and R. Wardle, 2015: Trends in the local Hadley and local Walker circulations. *Journal of Geophysical Research: Atmospheres*, **120**, no. 15, 7599–7618, doi:10.1002/2014JD022652.
- [203] Schwendike, J., P. Govekar, M. J. Reeder, R. Wardle, G. J. Berry, and C. Jakob, 2014: Local partitioning of the overturning circulation in the tropics and the connection to the hadley and walker circulations. *Journal of Geophysical Research: Atmospheres*, **119**, no. 3, 1322–1339.
- [204] Seidel, D. J., Q. Fu, W. J. Randel, and T. J. Reichler, 2008: Widening of the tropical belt in a changing climate. *Nature Geoscience*, **1**, 21–24, doi:10.1038/ngeo.2007.38.
- [205] Seo, K.-H., D. M. W. Frierson, and J.-H. Son, 2014: A mechanism for future changes in Hadley circulation strength in CMIP5 climate change simulations. *Geophysical Research Letters*, **41**, no. 14, 5251–5258, doi:10.1002/2014GL060868.
- [206] Seth, A., S. A. Rauscher, M. Rojas, A. Giannini, and S. J. Camargo, 2011: Enhanced spring convective barrier for monsoons in a warmer world? *Climatic Change*, **104**, 403–414, doi:10.1007/s10584-010-9973-8.
- [207] Shaw, T. A., 2014: On the role of planetary-scale waves in the abrupt seasonal transition of the Northern Hemisphere general circulation. *Journal of the Atmospheric Sciences*, **71**, no. 5, 1724–1746, doi:10.1175/JAS-D-13-0137.1.
- [208] Singh, M. S., 2019: Limits on the extent of the solsticial Hadley cell: The role of planetary rotation. *J. Atmos. Sci.*, **76**, 1989–2004, doi:10.1175/JAS-D-18-0341.1.
- [209] Singh, M. S. and Z. Kuang, 2016: Exploring the role of eddy momentum fluxes in determining the characteristics of the equinoctial Hadley circulation: fixed-SST simulations. *Journal of the Atmospheric Sciences*, **73**, no. 6, 2427–2444, doi:10.1175/JAS-D-15-0212.1.
- [210] Singh, M. S., Z. Kuang, and Y. Tian, 2017: Eddy influences on the strength of the Hadley circulation: dynamic and thermodynamic perspectives. *Journal of the Atmospheric Sciences*, **74**, no. 2, 467–486, doi:10.1175/JAS-D-16-0238.1.
- [211] Son, S.-W., E. P. Gerber, J. Perlwitz, L. M. Polvani, N. Gillett, K.-H. Seo, V. Eyring, T. G. Shepherd, D. Waugh, H. Akiyoshi, et al., 2010: Impact of stratospheric ozone on Southern Hemisphere circulation change: A multimodel assessment. *Journal of Geophysical Research*, **115**, no. D3, D00M07, doi:10.1029/2010JD014271.
- [212] Son, S.-W., S.-Y. Kim, and S.-K. Min, 2018: Widening of the Hadley cell from Last Glacial Maximum to future climate. *Journal of Climate*, **31**, no. 1, 267–281, doi:10.1175/JCLI-D-17-0328.1.
- [213] Son, S.-W., L. M. Polvani, D. W. Waugh, H. Akiyoshi, R. Garcia, D. Kinnison, S. Pawson, E. Rozanov, T. G. Shepherd, and K. Shibata, 2008: The impact of stratospheric ozone recovery on the Southern Hemisphere westerly jet. *Science*, **320**, no. 5882, 1486–1489, doi:10.1126/science.1155939.
- [214] Son, S.-W., L. M. Polvani, D. W. Waugh, T. Birner, H. Akiyoshi, R. R. Garcia, A. Gettelman, D. A. Plummer, and E. Rozanov, 2009: The impact of stratospheric ozone recovery on tropopause height trends. *Journal of Climate*, **22**, no. 2, 429–445, doi:10.1175/2008JCLI2215.1.

- [215] Staten, P. W., K. M. Grise, S. M. Davis, K. Karneauskas, and D. N., 2019: Regional widening of tropical overturning: Forced change, natural variability, and recent trends. *Journal of Geophysical Research: Atmospheres*, **124**, no. 12, 6104–6119, doi:10.1029/2018JD030100.
- [216] Staten, P. W., K. M. Grise, S. M. Davis, K. B. Karneauskas, D. W. Waugh, A. C. Maycock, Q. Fu, K. Cook, O. Adam, I. R. Simpson, R. J. Allen, K. Rosenlof, G. Chen, C. C. Ummenhofer, X.-W. Quan, J. P. Kossin, and S.-W. Davis, Nicholas A ando Son, 2020: Tropical widening: From global variations to regional impacts. *Bulletin of the American Meteorological Society*, **101**, no. 6, E897–E904, doi:10.1175/BAMS-D-19-0047.1.
- [217] Staten, P. W., J. Lu, K. M. Grise, D. S. M., and T. Birner, 2018: Re-examining tropical expansion. *Nature Climate Change*, **8**, 768–775, doi:10.1038/s41558-018-0246-2.
- [218] Staten, P. W. and T. Reichler, 2014: On the ratio between shifts in the eddy-driven jet and the Hadley cell edge. *Climate dynamics*, **42**, 1229–1242, doi:10.1007/s00382-013-1905-7.
- [219] Steptoe, H., L. Wilcox, and E. Highwood, 2016: Is there a robust effect of anthropogenic aerosols on the southern annular mode? *Journal of Geophysical Research: Atmospheres*, **121**, no. 17, 10–029.
- [220] Studholme, J. and S. Gulev, 2018: Concurrent Changes to Hadley Circulation and the meridional distribution of tropical cyclones. *Journal of Climate*, **31**, no. 11, 4367–4389, doi:10.1175/JCLI-D-17-0852.1.
- [221] Sun, L., G. Chen, and J. Lu, 2013: Sensitivities and mechanisms of the zonal mean atmospheric circulation response to tropical warming. *Journal of the Atmospheric Sciences*, **70**, no. 8, 2487–2504, doi:10.1175/JAS-D-12-0298.1.
- [222] Sun, Y., L. Z. X. Li, G. Ramstein, T. Zhou, N. Tan, M. Kageyama, and S. Wang, 2019: Regional meridional cells governing the interannual variability of the Hadley circulation in boreal winter. *Climate Dynamics*, **52**, 831–853, doi:10.1007/s00382-018-4263-7.
- [223] Tandon, N. F., E. P. Gerber, A. H. Sobel, and L. M. Polvani, 2013: Understanding Hadley cell expansion versus contraction: Insights from simplified models and implications for recent observations. *Journal of Climate*, **26**, no. 12, 4304–4321, doi:10.1175/JCLI-D-12-00598.1.
- [224] Tao, L., Y. Hu, and J. Liu, 2016: Anthropogenic forcing on the Hadley circulation in CMIP5 simulations. *Climate Dynamics*, **46**, no. 9–10, 3337–3350, doi:10.1007/s00382-015-2772-1.
- [225] Tosca, M., J. Randerson, and C. Zender, 2013: Global impact of smoke aerosols from landscape fires on climate and the hadley circulation. *Atmospheric Chemistry and Physics*, **13**, no. 10, 5227–5241.
- [226] Trenberth, K. E. and J. T. Fasullo, 2017: Atlantic meridional heat transports computed from balancing Earth's energy locally. *Geophysical Research Letters*, **44**, no. 4, 1919–1927, doi:10.1002/2016GL072475.
- [227] Trenberth, K. E., D. P. Stepaniak, and J. M. Caron, 2000: The global monsoon as seen through the divergent atmospheric circulation. *Journal of Climate*, **13**, no. 22, 3969–3993, doi:10.1175/1520-0442(2000)013<3969:TGMAS-T>2.0.CO;2.
- [228] Tziperman, E., M. E. Raymo, P. Huybers, and C. Wunsch, 2006: Consequences of pacing the Pleistocene 100 kyr ice ages by nonlinear phase locking to Milankovitch forcing. *Paleoceanography and Paleoclimatology*, **21**, no. 4, PA4206, doi:10.1029/2005PA001241.
- [229] Vallis, G. K., P. Zurita-Gotor, C. Cairns, and J. Kidston, 2015: Response of the large-scale structure of the atmosphere to global warming. *Quarterly Journal of the Royal Meteorological Society*, **141**, no. 690, 1479–1501, doi:10.1002/qj.2456.
- [230] Vecchi, G. A. and B. J. Soden, 2007: Global warming and the weakening of the tropical circulation. *Journal of Climate*, **20**, no. 17, 4316–4340, doi:10.1175/JCLI4258.1.
- [231] Voigt, A., R. Pincus, B. Stevens, S. Bony, O. Boucher, N. Bellouin, A. Lewinschal, B. Medeiros, Z. Wang, and H. Zhang, 2017: Fast and slow shifts of the zonal-mean intertropical convergence zone in response to an idealized anthropogenic aerosol. *Journal of Advances in Modeling Earth Systems*, **9**, no. 2, 870–892, doi:10.1002/2016MS000902.



- [232] Vuorela, L. A. and I. Tuominen, 1964: On the mean zonal and meridional circulations and the flux of moisture in the northern hemisphere during the summer season. *Pure and Applied Geophysics*, **57**, 167–180, doi:10.1007/BF00879722.
- [233] Walker, C. C. and T. Schneider, 2005: Response of idealized Hadley circulations to seasonally varying heating. *Geophysical Research Letters*, **32**, L06813, doi:10.1029/2004GL022304.
- [234] — 2006: Eddy influences on Hadley circulations: Simulations with an idealized GCM. *Journal of the Atmospheric Sciences*, **63**, 3333–3350, doi:10.1175/JAS3821.1.
- [235] Wang, C.-C., W.-L. Lee, and C. Chou, 2019: Climate effects of anthropogenic aerosol forcing on tropical precipitation and circulations. *Journal of Climate*, **32**, no. 16, 5275–5287, doi:10.1175/JCLI-D-18-0641.1.
- [236] Wang, H., S.-P. Xie, and Q. Liu, 2016: Comparison of climate response to anthropogenic aerosol versus greenhouse gas forcing: Distinct patterns. *Journal of Climate*, **29**, no. 14, 5175–5188, doi:10.1175/JCLI-D-16-0106.1.
- [237] Wang, H., S.-P. Xie, H. Tokinaga, Q. Liu, and Y. Kosaka, 2016: Detecting cross-equatorial wind change as a fingerprint of climate response to anthropogenic aerosol forcing. *Geophysical Research Letters*, **43**, no. 7, 3444–3450, doi:10.1002/2016GL068521.
- [238] Wang, H., S.-P. Xie, X.-T. Zheng, Y. Kosaka, Y. Xu, and Y.-F. Geng, 2020: Dynamics of southern hemisphere atmospheric circulation response to anthropogenic aerosol forcing. *Geophysical Research Letters*, **47**, no. 19, e2020GL089919, doi:10.1029/2020GL089919.
- [239] Wang, T., N. Wang, and D. Jiang, 2023: Last glacial maximum itcz changes from pmip3/4 simulations. *Journal of Geophysical Research: Atmospheres*, **128**, no. 10, e2022JD038103, doi:https://doi.org/10.1029/2022JD038103.
- [240] Watt-Meyer, O., D. M. Frierson, and Q. Fu, 2019: Hemispheric asymmetry of tropical expansion under co2 forcing. *Geophysical Research Letters*, **46**, no. 15, 9231–9240, doi:10.1029/2019GL083695.
- [241] Waugh, D. W., K. M. Grise, W. J. M. Seviour, S. M. Davis, N. Davis, O. Adam, S.-W. Son, I. R. Simpson, P. W. Staten, A. C. Maycock, et al., 2018: Revisiting the relationship among metrics of tropical expansion. *Journal of Climate*, **31**, no. 18, 7565–7581, doi:10.1175/JCLI-D-18-0108.1.
- [242] Williams, J., R. G. Barry, and W. M. Washington, 1974: Simulation of the atmospheric circulation using the NCAR global circulation model with ice age boundary conditions. *Journal of Applied Meteorology and Climatology*, **13**, no. 3, 305–317, doi:10.1175/1520-0450(1974)013<0305:SOTACU>2.0.CO;2.
- [243] Wills, R. C., X. J. Levine, and T. Schneider, 2017: Local energetic constraints on walker circulation strength. *Journal of the Atmospheric Sciences*, **74**, no. 6, 1907–1922, doi:10.1175/JAS-D-16-0219.1.
- [244] Wodzicki, K. R. and A. D. Rapp, 2016: Long-term characterization of the Pacific ITCZ using TRMM, GPCP, and ERA-Interim. *Journal of Geophysical Research: Atmospheres*, **121**, no. 7, 3153–3170, doi:10.1002/2015JD024458.
- [245] Xia, Y., Y. Hu, and J. Liu, 2020: Comparison of trends in the Hadley circulation between CMIP6 and CMIP5. *Science Bulletin*, **65**, no. 19, 1667–1674, doi:10.1016/j.scib.2020.06.011.
- [246] Xia, Y., Y. Wang, Y. Huang, Y. Hu, J. Bian, C. Zhao, and C. Sun, 2021: Significant contribution of stratospheric water vapor to the poleward expansion of the hadley circulation in autumn under greenhouse warming. *Geophysical Research Letters*, **48**, no. 17, e2021GL094008, doi:10.1029/2021GL094008.
- [247] Yoshioka, M., N. M. Mahowald, A. J. Conley, W. D. Collins, D. W. Fillmore, C. S. Zender, and D. B. Coleman, 2007: Impact of desert dust radiative forcing on sahel precipitation: Relative importance of dust compared to sea surface temperature variations, vegetation changes, and greenhouse gas warming. *Journal of Climate*, **20**, no. 8, 1445–1467.
- [248] Yu, J.-Y., C. Chou, and J. D. Neelin, 1998: Estimating the gross moist stability of the tropical atmosphere. *Journal of the atmospheric sciences*, **55**, no. 8, 1354–1372.

- 1388 [249] Yue, X., H. Liao, H. Wang, S. Li, and J. Tang, 2011: Role of sea surface temperature responses in simulation of the  
1389 climatic effect of mineral dust aerosol. *Atmospheric Chemistry and Physics*, **11**, no. 12, 6049–6062.
- 1390 [250] Yue, X., H. Wang, H. Liao, and D. Jiang, 2011: Simulation of the direct radiative effect of mineral dust aerosol on the  
1391 climate at the last glacial maximum. *Journal of Climate*, **24**, no. 3, 843–858.
- 1392 [251] Zanchettin, D., C. Timmreck, M. Khodri, A. Schmidt, M. Toohey, M. Abe, S. Bekki, J. Cole, S.-W. Fang, W. Feng, et al.,  
1393 2021: Effects of forcing differences and initial conditions on inter-model agreement in the volmip volc-pinatubo-full  
1394 experiment. *Geoscientific Model Development Discussions*, 1–39, doi:10.5194/gmd-2021-372.
- 1395 [252] Zaplotnik, Ž., M. Pikovnik, and L. Boljka, 2022: Recent hadley circulation strengthening: a trend or multidecadal vari-  
1396 ability? *Journal of Climate*, **35**, no. 13, 4157–4176.
- 1397 [253] Zhou, Y. P., K.-M. Xu, Y. C. Sud, and A. K. Betts, 2011: Recent trends of the tropical hydrological cycle inferred from  
1398 Global Precipitation Climatology Project and International Satellite Cloud Climatology Project data. *Journal of Geophys-  
1399 ical Research: Atmospheres*, **116**, no. D9, D09101, doi:10.1029/2010JD015197.